

# ACDC project – Autonomously Controlled Distributed Chargers
# Final report

**Marinelli, Mattia; Striani, Simone; Pedersen, Kristoffer Laust; Sevdari, Kristian; Hach, Maria; Mikkelsen, Oliver Lund; Rakowski, Marcin**

*Publication date:*
2023

*Document Version*
Publisher's PDF, also known as Version of record

# ACDC project (Autonomously Controlled Distributed Chargers) Final report

## 1. Project details

| | |
|---|---|
| **Project title** | ACDC – Autonomously Controlled Distributed Chargers |
| **File no.** | 64019-0541 |
| **Name of the funding scheme** | 2019 II - Systemintegration |
| **Project managing company / institution** | DTU Wind and Energy Systems |
| **CVR number** (central business register) | DTU: 30 06 09 46 |
| **Project partners** | Nissan (NIS); Circle Consult (CC); Trefor El net øst (ENØ); Vestas (VES); Bornholms Energi & Forsyning (BEOF) |
| **Submission date** | 14 December 2023 |
| **Authors** | DTU: Mattia Marinelli, Simone Striani, Kristoffer L. Pedersen, Kristian Sevdari;<br>BEOF: Maria Hach<br>Circle Consult: Oliver Lund Mikkelsen<br>Nissan: Marcin Rakowski |

# 2. Summary

## 2.1 English

The government wants to suspend the sale of all diesel and gasoline cars in Denmark by 2030. By that time, it is reasonable to expect between 0.5 and 1 million electric vehicles on the road. Controlling the charging process of one million vehicles can provide large flexibility to the electricity system and support the integration of more renewable sources. However, the control infrastructure behind the chargers needs to be sufficiently simple and cost-effective in order to make the process both technically and economically successful. Ideally, the process must become autonomous.

The ACDC project developed two new technologies: an electric vehicle autonomous smart charge controller and a virtual aggregator. The autonomous charge controls a set of electric vehicles charge in order to ensure the fulfillment of specific grid services. The virtual aggregator broadcasts a signal to the set of autonomous chargers in order to coordinate their action. Both technologies are developed and demonstrated in the project by using up to 5 vehicles in Risø campus and up to 20 vehicles in Bornholm. Simultaneously with the development of the hardware, power systems stability studies are performed to analyze the effect of aggregated charging on the large scale.

## 2.2 Danish

Regeringen vil stoppe salget af diesel- og benzinbiler i 2030. På det tidspunkt er det forventet at der allerede er mellem en halv og en hel million elbiler på vejene. Ved at styre opladningen kan en million elbiler levere en meget stor mængde fleksibilitet til elnettet og hjælpe med at bruge en større mængde af vedvarende energi. Styringen af opladningen er nødt til at være både simpel og billig, hvis det skal lykkedes at implementere det ud fra et både teknisk og økonomisk synspunkt. Ideelt set skal ladestanderne agere helt autonomt.

ACDC projektet udviklede to ny teknologier: en autonom elbilsladestander og en virtuel aggregator. De autonome ladere skal hver især styre opladningen af en elbil på en måde hvor de leverer nogle specifikke netydelser. Den virtuelle aggregator sender et enkelt signal til alle ladestanderne for at koordinere deres opladning. Begge teknologier blev udviklet og demonstreret i løbet af projektet med 5 elbiler på Risø campus og op til 20 elbiler på Bornholm. Samtidig med udviklingen af hardwaren blev der udført stabilitetsstudier på hele elnettet for at undersøge hvilken effekt aggregeret ladning havde i stor skala.

# *3.* Project objectives

The overarching objective of the project is to demonstrate that it is possible to control autonomously a set of distributed chargers in order to replicate the functionality of an aggregated set of centrally controlled chargers providing grid services. The comparison is based on both technical and economic angles. Specifically, the technical perspective validated the fulfillment of grid requirements in term of voltage, current and frequency. The economic sustainability of the solution was investigated in order to assess whether it is more convenient, and therefore more likely to succeed, compared to the traditional centralized approach.

The project main objectives are listed below:

-) Autonomous and coordinated charging control without detailed information exchange

-) One way – slow speed – communication to the car (brand-agnostic)

-) Development of new technologies according to the IEC standard (can be used with any EV)

-) Adaptive algorithms according to grid states and EV population size

-) Behind-the-meter operation in order to avoid grid reinforcement

-) Possibility to provide fast grid services

The following research questions drove the scientific investigation:

- How does the stochasticity in the usage of EVs influence the control strategy when providing services to the power systems?
- How to cluster heterogeneous sets of small domestic controllable units so that their controlling capability resemble the one of a large power plant?
- Will the autonomous control of EVs initiate large-scale instabilities into the grid?

The research content of the project was streamlined in the following three areas.

1. Architecture for autonomous chargers. The current centralized approach for controlling EVs may well serve the purpose of providing grid services, but it adds complexity and costs, making the whole solution potentially not feasible (from an economic perspective). On the other hand, it is necessary to specify the way we are delegating to the charger the decision on how much and how quickly to react. It is therefore necessary to specify the necessary information flow to make sure that the requested controlling actions are realized.

2. Large-scale management of clusters of electric vehicles. There has been extensive work in modelling EVs; nonetheless, gaps remain in accurate models especially when it comes to understanding the aggregated response of heterogeneous clustering of such units over different areas. The main challenge arises by the fact that their main function is not to serve the power system, but instead the private owner.

3. Power smoothing applications. This area would include set-up involving consumers as well as coupling with wind power plants (as hybrid-power plants). Compared to the previous investigation area that has a system-angle, the focus here lies on the local application. The scientific value resides in defining proper control strategies for providing short term balancing of the local consumption (or production) and ensure a controllable power output.

# 4. Project implementation

## 4.1 Evolution of the project

The project was structured in 6 work packages as shown in Figure 1. The most critical aspect of the evolution of the ACDC charger was the hardware development, which resulted in more complicated than initially assessed also due to the consequences on the supply chain of electronic components following the Corona pandemic. Although some activities have been delayed and revised to fit the current possibilities, the partners managed to fulfill the key objectives set at the beginning of the project. Eventually the hardware was developed in time for having extensive lab controllers' validation and therefore for the field demonstration closing the project.

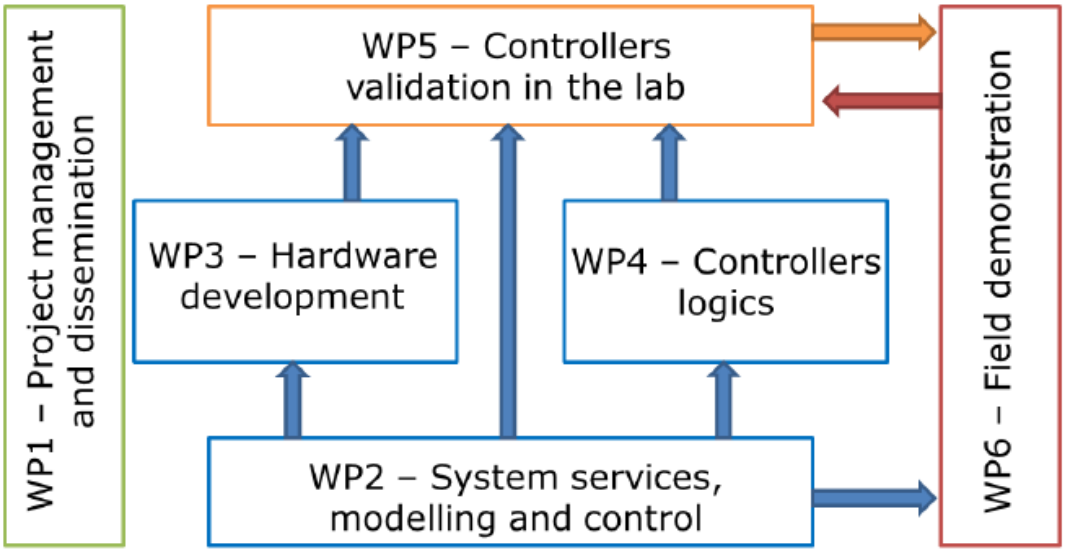


Figure 1: Subtasks of the ACDC project.

## 4.2 Risks associated

The foreseen risks associated with conducting the project are summarized in Table 1. As predicted, the development of the charger's hardware was a very time consuming task due to the many function associated with the charger, both mechanical and electrical. The other most probable risk was not to have standards supporting the use of such charger. This risk was apparently overestimated because there were no challenging obstacles in this domain.

Table 1: Foreseen risks associated with conducting the project.

| Risk | Probability | Effect | Mitigation measures |
|---|---|---|---|
| Risk 1: autonomous charger not developed in time | Medium | Without the autonomous charge controller ready, only simulations can be run | Establish a clear development plan with clear milestones (see WP3 description) |
| Risk 2: WiFi communication not doable | Low | With no WiFi, only normal charging is allowed | Ensure proper WiFi coverage |
| Risk 3: no standard supporting technical aspects | High | Some functionality may not available | Give input to the standardization committee and disseminate results to IEC |
| Risk 4. Inability to provide grid services due to departure of designed system from planned performance | Low | Since most parts has been tested in labs, the risk is low, but if not, the system has no effect and no value. | Stick with the plan |

## 4.3 Milestone reached

The original milestones where the following:

1) List of I/O of charge controller and virtual aggregator HW and SW (by month 12). Modeling of the first use case: prove by simulations that the concept is working.
2) Physical tests of the hardware into the lab which will provide input for a revision of the hardware specifications (by month 24)
3) Tests into the field of the (revised) HW and plan for commercialization (by month 36).

All of the above-mentioned milestones were successfully reached. The system is now deployed in DTU Risø campus and at BEOF facility in Rønne. Additionally, we have models to simulate further large-scale adoption of the technology.

# 5. Project results

## 5.1 Overview of research results

The project tackled the following research directions:

- Definition and assessment of charging flexibility from clusters of electric vehicles.
- Testing of on-board chargers to quantify flexibility potential and charging efficiency.
- Development of autonomous and distributed charging technologies.
- Architecture definition and controlling logics.
- Controllers validation in real conditions and Lab demonstration.

## 5.2 Definition and assessment of charging flexibility from clusters of electric vehicles

The transportation and power sectors are experiencing a paradigm shift. On the one hand, the transition away from fossil fuels in the transportation sector is paving the way for the emergence of electric mobility. On the other hand, the shift towards a sustainable power system necessitates novel approaches to power system operation and planning. Therefore, a synergy between electric mobility and renewable energy sources (RESs) can contribute significantly to the progress of both industries. In this context, the charging infrastructure serves as the link between the transportation and power sectors, encompassing both electrical and communication aspects. The prospects and hurdles of electrifying transportation hinge on the positioning, variety, utilization, and functionalities of this charging infrastructure.

To date, slow charging is by far the most widely utilized type of charging infrastructure for public and private charging sessions. Here, slow charging correlates with long vehicle parking times, allowing for better accommodating the charging energy demand in combination with the restrictions of the power grid.

All the services required from the perspective of the power system fall under ancillary services. These account for all the services offered in the balancing and flexibility markets. Frequency services maintain the system-wide frequency characteristic, while the flexibility services assist local challenges. While for frequency services there is an available market framework, the flexibility services are lacking, or rather we are currently in the first steps of the implementation of such markets. The literature agrees on the allocation of flexibility services based on five features: resource type, duration, incentives, location, and enablers. Therefore, the authors propose the following definition for flexibility services:

***Flexibility service refers to scheduling and/or modulation of the collective/single consumption or generation of electrical appliances or distributed technologies. This is performed in agreement with the customer (consumer or generator) and following the grid code, as a response to signals from market enablers, in order to increase the network reliability and efficiency at a predefined time and location.***

### 5.2.1 Flexibility services

Flexibility services are grouped into three categories: natural, scheduled, and conditional. Natural flexibility services refer to actions actively enabled by the system operator (SO) without the need for a procurement process, namely demand response programs, control of network components and grid code requirements. Scheduled services account for measures procured by the SOs to not jeopardize system safety operation or counteract N-1 situations. Conditional flexibility services are activated to restore system stability or increase power system efficiency. The difference between conditional and scheduled services is the activation type. For

conditional services the activation is post-event, whereas for scheduled services it is a pre-event or during event activation. ”Natural” flexibility comes first, it is a tool based on the agreement with the user only, and it potentially reaches the highest number of flexibility providers, along the timeline. If natural flexibility is not enough, ”scheduled” flexibility is used by SO in a dedicated area, with a specific timeline and fewer providers. Similarly, ”conditional” flexibility is the last resource to avoid further escalation of the problem or help the system recover. Five major topics are recognized: congestion management, voltage regulation, power quality, grid stability, and emission (CO2) management.

***Congestion management*** refers to the measures taken by SO to maintain the desired loading on their network components, such as transformers and electric lines. The reasons for doing so are twofold: i) high overloading of a grid component will instantly damage the component and ii) moderate overloading will produce heat higher than normal from the current flowing through the device. With time, extra heat shortens the lifetime of the device, requiring earlier maintenance.

***Voltage regulation*** refers to measures taken from SO to maintain voltage stability and overcome short-circuit scenarios. Here, the paper distinguishes between voltage and reactive power support. In the former, both active and reactive power play a role, while the latter is more related to reactive power support with a focus on weak grids. The cause of voltage instability derives from the fact that the power network is operated close to stability limits and different load characteristics may trigger fluctuations in the voltage profiles.

***Power quality*** refers to the measures taken from distribution system operator (DSO) to improve supply quality and reduce grid operational losses. Here, the voltage regulation service is distinguished from the power quality service because it belongs to both DSO and transmission system operator (TSO). In contrast, the latter belongs to the DSO. Besides, voltage regulation itself has become quite important; hence, it deserves to be mentioned separately. Power quality is focused on the fast dynamics of switching of electronic devices, the mitigation of DERs, power flickers and the control of the end-user power factor.

***Grid stability*** services cover the power system stability, adequacy, and security of supply outside of the wholesale electricity and balancing markets and are operated by DSO and TSO. Services such as low-voltage/fault ride through, power factor control and anti-islanding are generally capabilities mandated in the grid code. In a high integration scenario of RESs, RESs power smoothing services might be required to operate the system safely and preserve frequency power reserves. Similarly, energy arbitrage and seasonal balancing are believed to be necessary services to cope with the unpredictability of RESs. In addition, emergency power and black-start capability are programmed for blackouts (according to ENTSO-E), or to provide emergency power to areas affected by local emergencies.

As the name suggests, ***emission management*** relates to a demand response service type of use (TyoU) that intends to avoid RESs spilling and reduce consumption from polluting generators. The TyoU induces fees for the carbon intensity depending on the generation mix. Higher fees correlate with high-polluting generators.

Flexibility services are provided in the active and reactive power domains. Recognizing the literature recommendations and the novel applications of commercial flexibility stakeholders are only looking at active power services, mainly congestion management. In the short term, possible commercial flexibility services are demand response programs, TyoU, valley filling, and peak shaving actions. In the long run, with high penetrations of EVs, other flexibility services such as phase balancing, power matching, and voltage regulation actions could be required.

### 5.2.2 Charging clusters and e-mobility flexibility map

The scientific literature distinguishes between "destination charging" and "charging destination". In the first, charging is complementary to other user needs, such as going to the supermarket, while in the second, charging drives the choice of user needs.

Furthermore, charging behaviors are reflected at different charging sites: i) home and public residential charging; ii) curbside and semi-public charging; iii) workplace charging; iv) fleet charging; v) large semi-public charging; vi) fast (en route) charging; vii) special semi-public charging; viii) charging forecourts; ix) semi-private charging and x) charging hubs. Although it is still quite early for the clusters to mature, the charging clusters derived from the review are in line with the clusters used in Working Group 4 of the IEA GEF Global e-mobility program. Consequently, *Figure 2* illustrates with examples the charging site operator (CSO), which is the representative of the cluster. The CSO can incorporate one charger, in the case of a home charger, or include multiple chargers, such as the charging forecourts. The higher the site hierarchy, the fewer chargers there are, while the site connection capacity increases. Furthermore, it is a challenging task to estimate the number of chargers in each cluster. This factor is one of the current limitations on forecasting flexibility of charging clusters. In addition, the charging technology needs to be mature before trying any estimation.

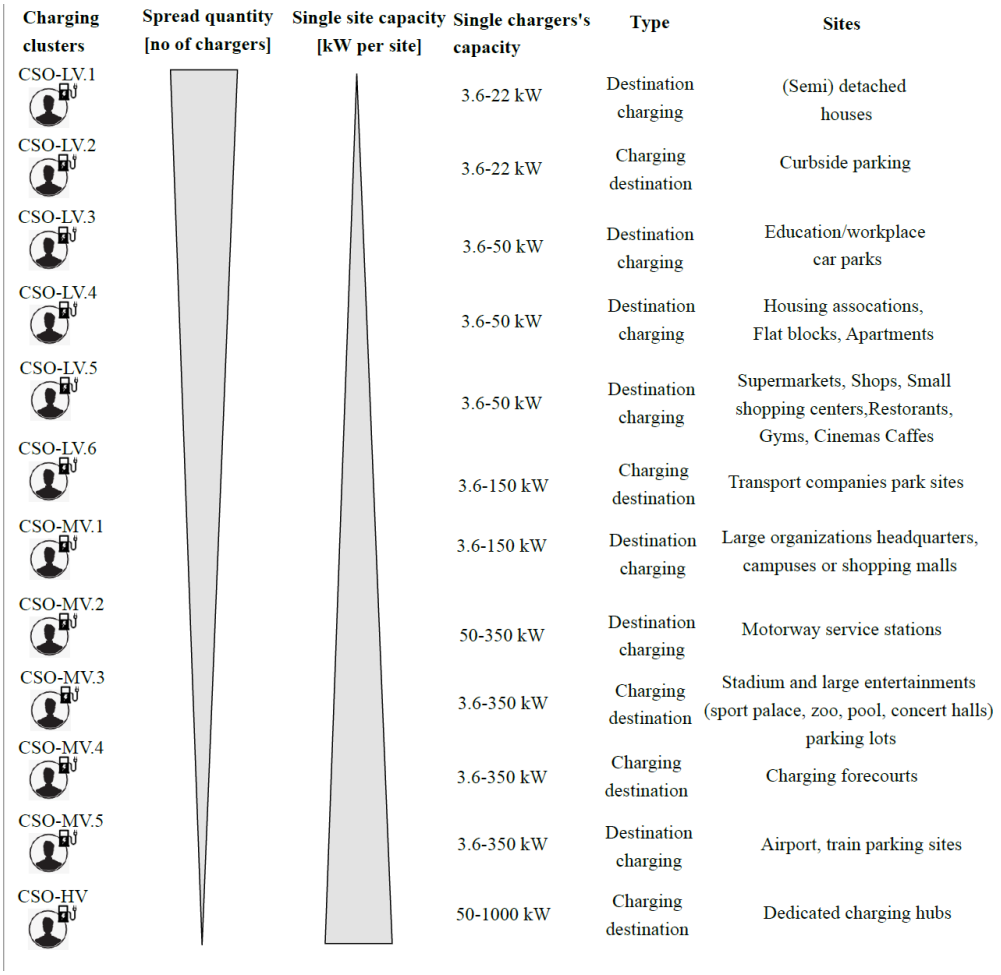


*Figure 2. Electric vehicle charging clusters.*

After identifying the charging clusters or CSOs, *Figure 3* matches the charging clusters with their grid location (low/medium/high voltage). Besides, it couples CSOs with possible delivery of flexibility and frequency services. This is achieved by matching the previously discussed ancillary services depending on V1G or V2G.

The V1G represents a smart load, while V2G (converter technology) is similar to battery energy storage. Furthermore, the drawing in *Figure 3* pairs each CSOs with the charging technology (AC and DC smart chargers) and with different EVs ownership types (passenger cars, taxis and fleets, autonomous vehicles, shuttles, and public transport buses).

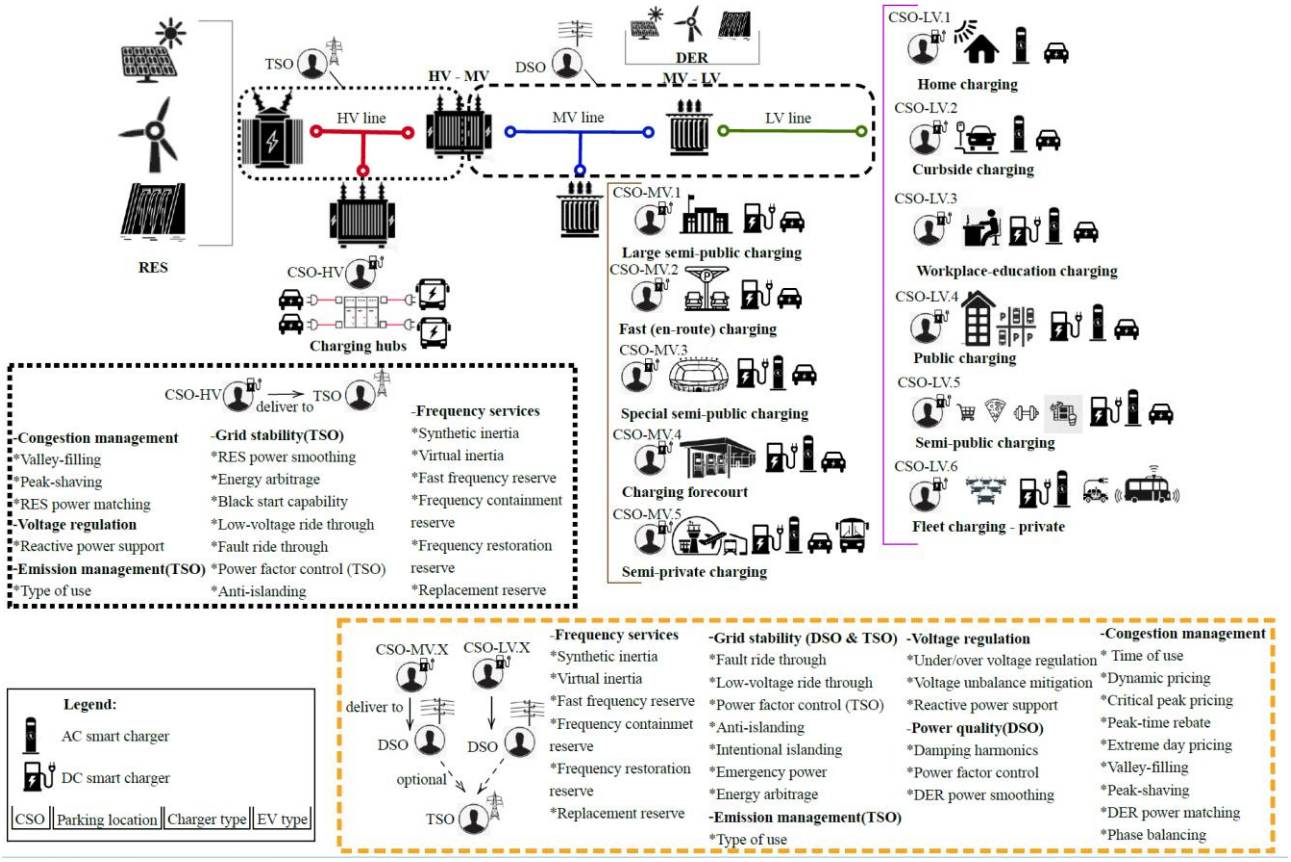


*Figure 3. E-mobility flexibility map.*

Overall, five out of eight frequency services and 26 out of 32 flexibility services can be provided by EVs. However, in three out of eight frequency services only, the charging technology is on a commercial stage. Similarly to what happens for flexibility services, congestion management services are mostly being developed for commercial applications.

### 5.2.3 **Flexibility framework**

*Figure 4* a) displays the flexibility architecture with all stakeholders, namely the EV-user, the CSO, the CPO, the aggregator, the energy community, the DSO, the TSO, and the flexibility platform. The EV-user provides consent of using its flexibility to the CSO. The CSO is the first flexibility provider. Furthermore, the CSOs require an infrastructure to operate, namely the EV charger. The CSOs are supplied from charger manufacturers and can operate the infrastructure on their own or delegate it to someone else. Here, the CPOs concept is introduced, which can control (back-end control) the charging infrastructure. A CPO can interface with one or multiple CSOs accordingly to the CSO desires. On the one hand, the CPO can deliver bilateral flexibility service to the SO. On the other hand, CPO can delegate front-end control (API interface) to an aggregator or an energy community to participate in the flexibility market. In this case, a larger entity is created, and CPO can help the process by providing flexibility forecasts of their sites to the aggregator or energy communities.

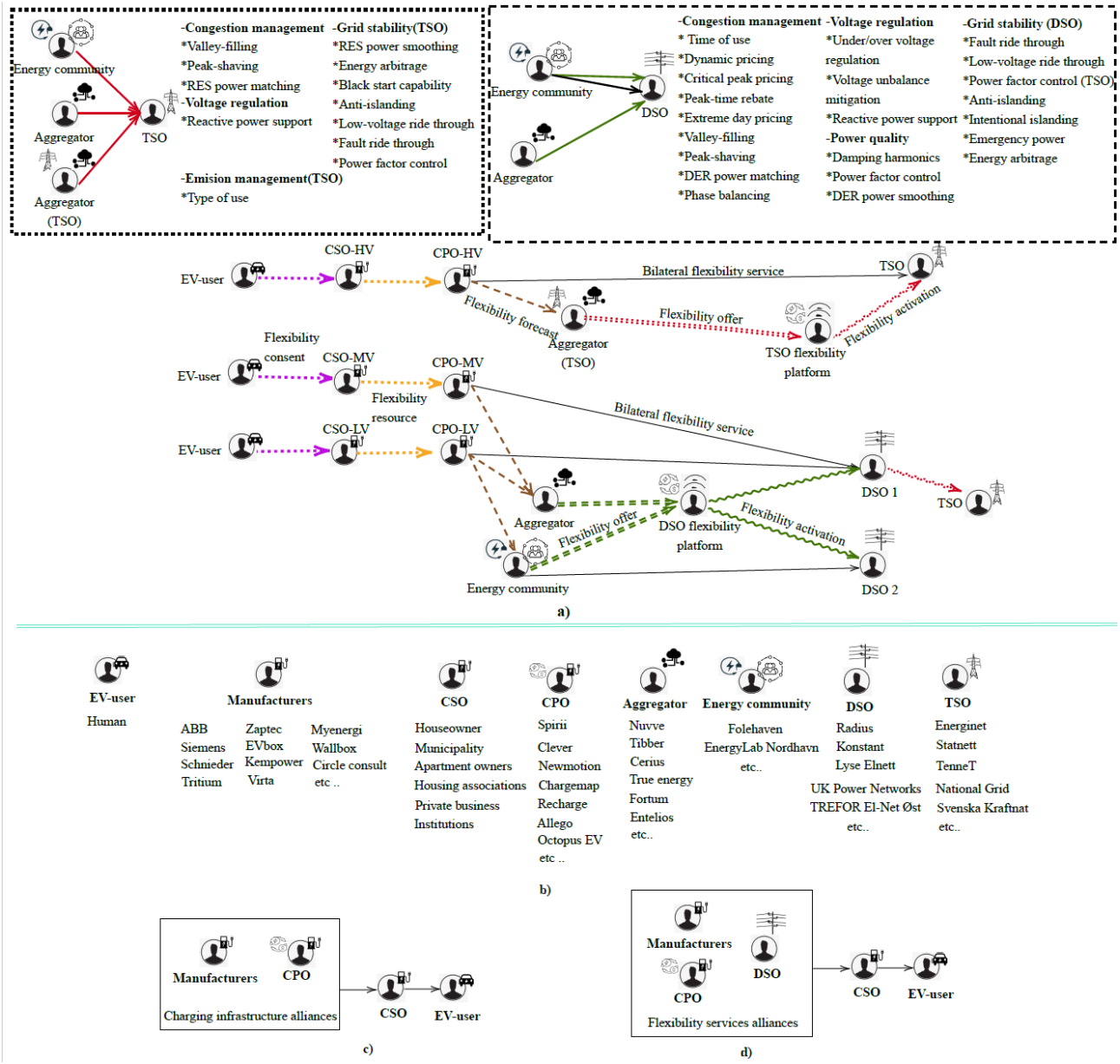


*Figure 4. a) Flexibility services architecture. b) The EVs flexibility supply chain. c) Charging infrastructure alliances. d) Flexibility services alliances. Examples are provided for the Nordic countries cases.*

Subsequently, the aggregator or energy communities bid a flexibility offer in the flexibility platform related to the DSOs or TSO network. The platform decides the winning bids and activates the flexibility service. Consequently, in *Figure 4* a) a summary of the flexibility services from the aggregating entity is presented. Furthermore, *Figure 4* b) illustrates the supply chain of flexibility services provided by EVs, including examples from the Nordic countries. In addition, one can distinguish the actors in e-mobility domain.

## 5.3 Testing of on-board chargers to quantify charging efficiency

### 5.3.1 AC charging technology

The realm of EVs has evolved in the recent years, with a notable focus on the charging technology. The development and deployment of EVSE for alternating current (AC) charging played a pivotal role in shaping the infrastructure for electric vehicles. This infrastructure encompasses the charging stations, connectors, and associated technologies that facilitate the transfer of electrical energy from the grid to the EV's battery. Understanding the nuances of AC charging technology is essential to understand the efficient and convenient charging options available to EV owners. In this section, we discuss the fundamental aspects, benefits, and challenges associated with the AC charging technology for EVs. The components required for AC charging are: i) EVSE, ii) Type 2 cable, and iii) EV.

*Figure 5* presents a detailed explanation of the components. When an EV is connected to an AC charging station, the OBC within the vehicle converts the incoming AC power to direct current (DC) to recharge the battery. EVSE is responsible for communicating, via the charging cable, the maximum charge current allowed to the vehicle. However, it is the EV battery management system (BMS) that controls the OBC operation and decides the final charging current according to the needs of the battery pack. Therefore, two technologies are central for controlling the AC charging process, the OBC and the EVSE.

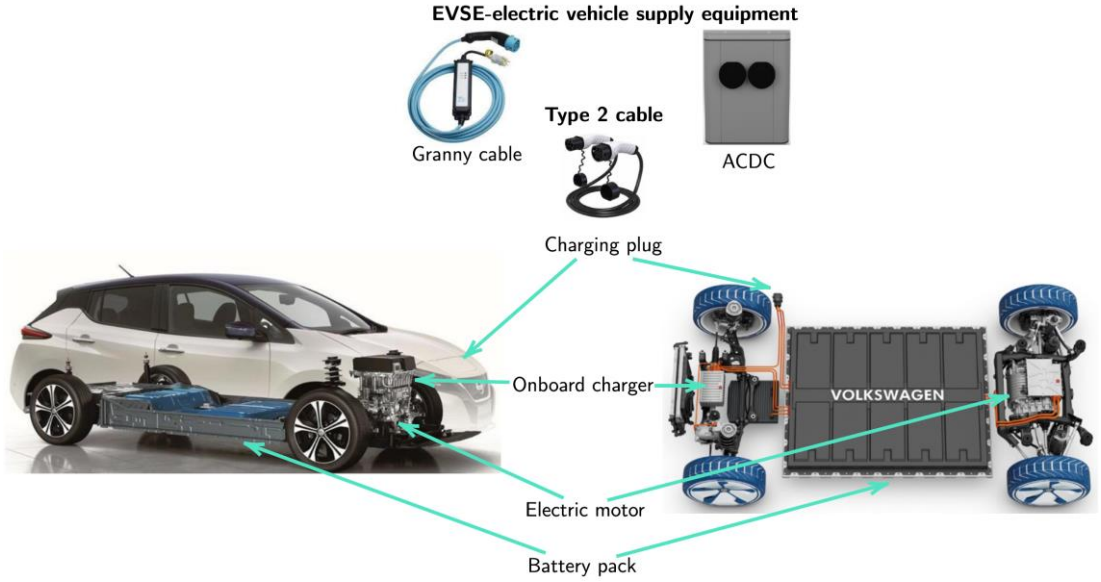


*Figure 5. EV AC charging technology overview.*

Two types of onboard chargers are present. The first one is the "dedicated" OBC, built as a standalone unit for the purpose of supplying the high-voltage battery pack and vehicle auxiliaries. The second one is the "integrated" OBC, which is combined to the electric motor of the vehicle. Here, the electric motor windings serve as an inductor for the OBC. The "dedicated" technology is more widespread than the "integrated" one.

### 5.3.2 **Onboard charger efficiency and reactive power draw**

A review of the literature highlights the lack of tested AC-to-DC conversion efficiency values for EV OBCs, albeit the most energy-intensive load in the household. Such conversion efficiency values from AC to DC are critical for the optimal large and small-scale management of charging strategies for EVs, life cycle assessment [87] and understanding the global energy implications of charging demand. The knowledge gap for OBC efficiency is even acknowledged by the European Commission in the European efficiency labeling regulation.

Figure 6 illustrates the results in the form of parabolic efficiency during standard smart charging for three-phase vehicles. The results also indicate a consistent improvement in efficiency from 2011 to 2022 at all charging current values.

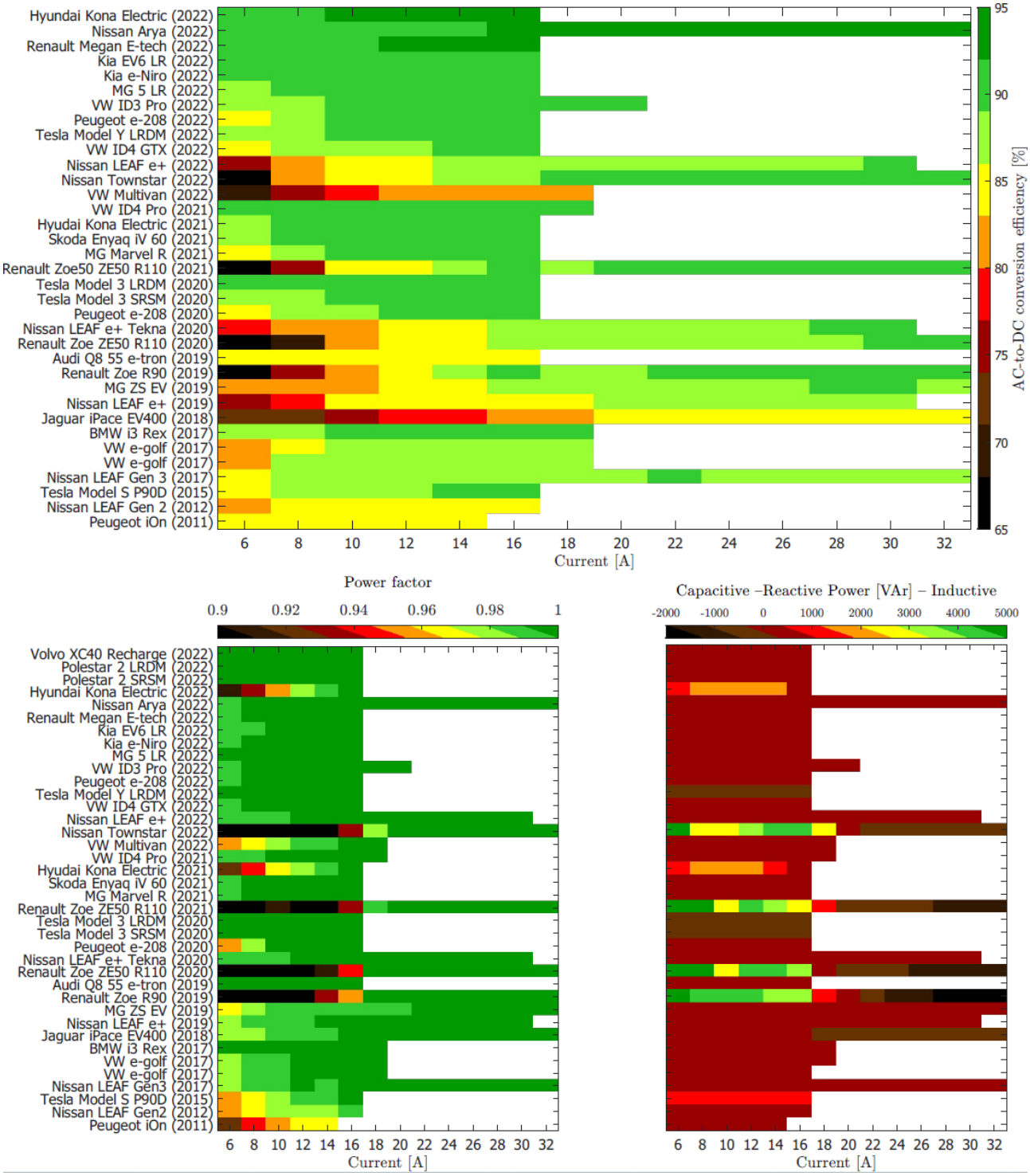


Figure 6. EV OBC characteristics. Top) AC-to-DC conversion efficiency. Bottom left) PF. Bottom right) Reactive powe consumption from 2011 to 2022.

The finding illustrated in Fig. 3.2 suggests a correlation between lower PF values and higher reactive power consumption. During low-current charging, some models violate the regulations pertaining to low-voltage grid demand connection, and several models exhibit substantial reactive power consumption. Consequently, there is a pressing need to reconsider the regulations concerning such high levels of reactive power consumption, as it poses a potential threat to the integrity of the low-voltage grid. Additionally, the data concerning reactive power reveal six distinct clusters of reactive power consumption curves. Clusters 1-5 represent behaviors of

dedicated OBC, which is the majority of the automotive industry. Most of EVs, spanning from early to the most recent models, consume reactive power within the range of 200-700 VAr, following a similar pattern to the Polestar 2 Long Range Dual-Motor (LRDM) (cluster 1). In general, the cluster's reactive power consumption diminishes as the charging current increases.

In contrast, the Tesla Model S P90D (400 V battery architecture) and the Kia EV6 LR (800 V battery architecture) represent the typical charging behavior of clusters 2 and 3, respectively, showcasing an increasing trend in reactive power consumption as the charging current increases. Consequently, this behavior cannot be solely attributed to a specific battery voltage architecture (400 or 800V), as it can be found in both architectures. Hyundai Kona represents cluster 4, characterized by an almost complete parabolic pattern of charging behavior. Within this cluster, the highest levels of reactive power consumption occur in the mid-range of charging current (between 10-12 Amps). In contrast, Tesla Models 3/Y represent the charging behavior of cluster 5, showing a negligible reactive power consumption (around 0 VAr). Lastly, cluster 6 encompasses EVs with an atypical level of reactive power consumption which employ a similar OBC as the Renault Chameleon/Zoe (integrated OBC with the electric motor).

### 5.3.3 **Optimizing smart charging**

The possibility of curtailing three-phase charging opens up the opportunity to better optimize charging operation in parking lots, fleets, or clusters controlled by an aggregator. Such a strategy has as its objective the fulfilment of the required energy demand (in kWh) without compromising the grid capacity connection (in kW) and the allowed consumption of reactive power (in kVAr). Grid connection capacity is generally the biggest constraint for charge-point operators. Therefore, smart charging is employed to maintain the acquired grid connection capacity from the DSO. However, modulating the charging current has additional implications for the OBC efficiency, as shown in *Figure 7*.

The OBC efficiency results can be clustered into six patterns.

1. Vehicles that charge with 16 Amps in three-phase (11.04 kW) and single-phase (3.68 kW) (cluster representative Skoda Enyaq iV 60). The efficiency of single-phase charging is lower than three-phase charging.
2. Vehicles that charge with 16 Amps in three-phase (11.04 kW) and single-phase (3.68 kW) (cluster representative Hyundai Kona Electric). The efficiency of single-phase charging above 14 Amps (3.22 kW) is higher than the efficiency of three-phase charging below 8 Amps (5.52 kW).
3. Vehicles that charge with 32 Amps in three-phase (22.08 kW) and single-phase (7.36 kW) (cluster representative Renault Zoe ZE50 R110). The efficiency of single-phase charging greater than 16 Amps (3.68 kW) is higher than the efficiency of three-phase charging below 12 Amps (8.28 kW).
4. Vehicles that charge with 16 Amps in three-phase (11.04 kW) and 32 Amps in single-phase (7.36 kW) (cluster representative Kia e-Niro). The efficiency of single-phase charging is lower than three-phase charging.
5. Vehicles that charge with 16 Amps in three-phase (11.04 kW) and 32 Amps in single-phase (7.36 kW) (cluster representative Peugeot e-208). The efficiency of single-phase charging is sometimes better than that of three-phase charging.
6. Vehicles that charge with 32 Amps in three-phase (22.08 kW) and single-phase (7.36 kW) (cluster representative Nissan Ariya). The efficiency of single-phase charging is lower than three-phase charging.

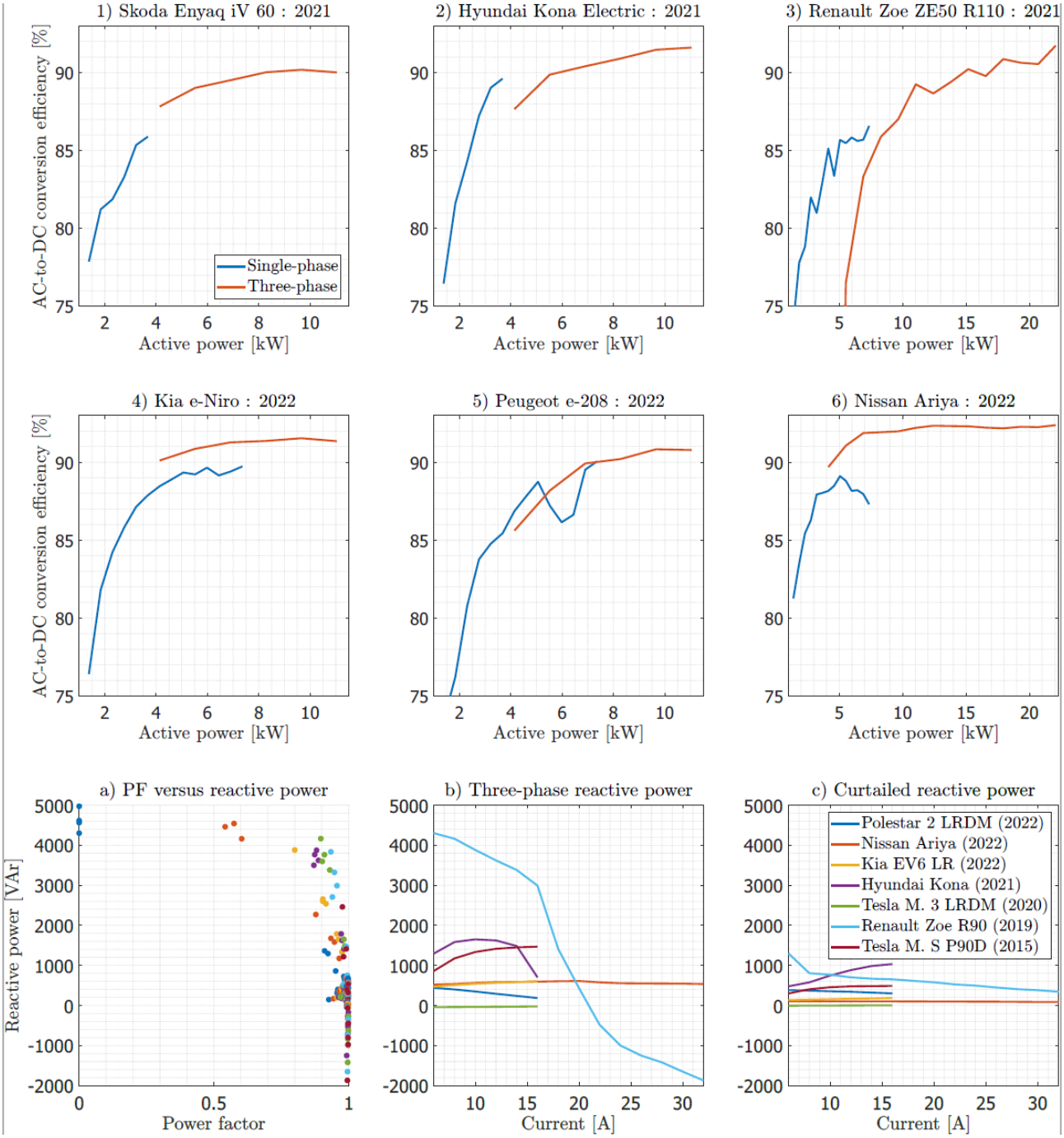


*Figure 7. Comparison of OBC efficiency between clusters of single-phase curtailed and a three-phase charger (1-6). Depending on which efficiency pattern the vehicle belongs to, the charging process can be optimized by looking at such efficiency curves. The correlation between lower PF and higher reactive power consumption a). Seven patterns of b) three-phase reactive power consumption are experienced similarly during c) curtailed reactive power consumption.*

Moreover, the viability of curtailed charging should be carefully analyzed by also considering the reactive power consumption. *Figure 7* a), b) and c) introduce the pattern of reactive power consumption for curtailed charging. Similarly to three-phase charging, there are six typical curves for curtailed charging. However, two patterns

behave differently, specifically Hyundai Kona and Renault Zoe. Finally, when curtailed charging is considered, the three-phase reactive power is not equal to that of three single-phase charging. Here, there are two options:

1. Lower reactive power consumption. For example, Kia EV6 Long Range (LR) consumes 471-606 VAr in three-phase charging. However, it consumes 135-186 VAr in curtailed charging. Therefore, 3 x (135 to 186) [VAr] < (471 to 606) [VAr].
2. Higher reactive power consumption. For example, polestar 2 SRSM consumes 442-183 VAr in three-phase charging. However, it consumes 368-257 VAr in curtailed charging. Therefore, 3 x (368 to 257)[VAr] > (442 to 183)[VAr].

Lastly, when looking for trends in the behavior of the OBC, the vehicle's SOC does not affect the efficiency of the OBC or reactive power consumption. This result confirms that the SOC only affects the amplitude of the charging current requested by the OBC. For example, a charging current of 10 Amps has the same efficiency and reactive power consumption at low (i.e. 40%) and high (i.e. 92%) SOC. In summary, the results show that decision-making for efficient smart charging should be made based on the individual vehicle model. CPOs can benefit from curtailed charging by better utilizing the available grid capacity; however, curtailed charging can reduce power quality by increasing reactive power consumption.

### 5.3.4 Current and future OBC performance conundrum

So far, small- or large-scale energy simulation models do not consider OBC efficiency. The results presented in this manuscript highlight the importance of considering such an approach. Depending on the level of modulation required, smart charging could increase the charging energy demand from 1-10 %. Furthermore, the testing campaign showed that efficiency varies between years and vehicle models. These curves are suggested to be implemented on large-scale simulations as a lookup table; otherwise, for better dynamics, every vehicle should be modelled according to the data presented in this paper. However, it is acknowledged that such a method can be computationally heavy. Thus, a more generalized approach is proposed in *Figure 8*. Based on the test results, a second-order polynomial is fitted for three-phase, curtailed, and single-phase vehicles. Such polynomials can be replicated to calculate the energy efficiency of EVs in an aggregated manner or for large-scale simulations.

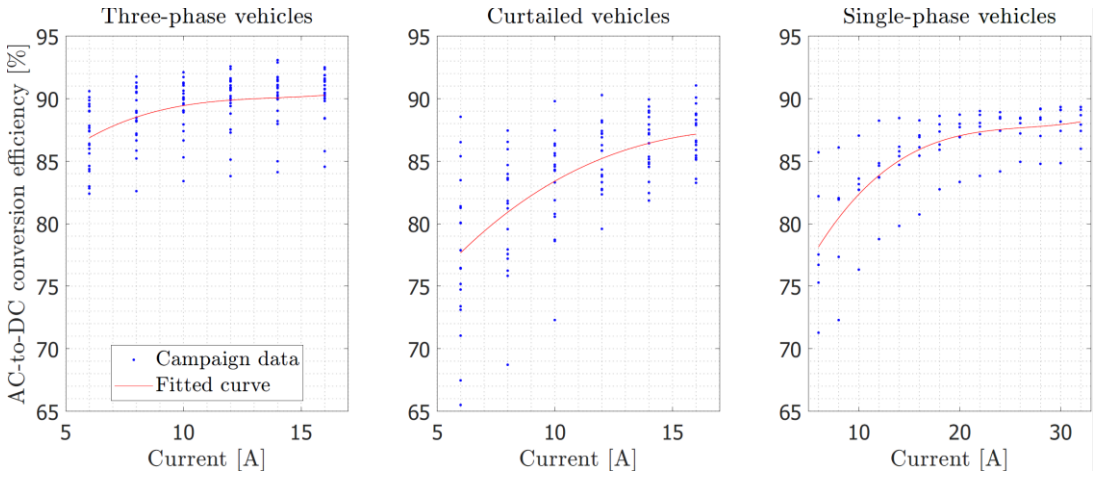


*Figure 8. Efficiency curves fitted to the data obtained from the testing campaign for left) three-phase, center) curtailed, and right) single-phase vehicles.*

In *Figure 9* a) and b) historical efficiency data are plotted alongside a second-order fitted function. As can be seen, the OBC maximum efficiency has progressed over the years. For 2022 the average efficiency is 90%, while the OBC minimum efficiency lies around 83%. Based on 11 years of data, a second-order polynomial prediction of efficiency is displayed up to 2040. The prediction considers a conservative approach, in which

the technology will develop at a faster rate until it saturates at a 96% efficiency value in 2035. These saturation levels for the development of OBC efficiency align with historical developments in solar inverters, which are a good example of technological progress. Therefore, earliest by 2030 it could be possible to reach a maximum OBC efficiency of 95% as a market average product. Similarly, by 2030 it could be possible to support a value of 88% for the minimum efficiency of OBC and a saturation of efficiency of 90% in 2035. The data suggest that the fleet of EVs varies considerably in its efficiency values. This uncertainty complicates the optimization of EVs; therefore, it needs to be addressed with technological improvements.

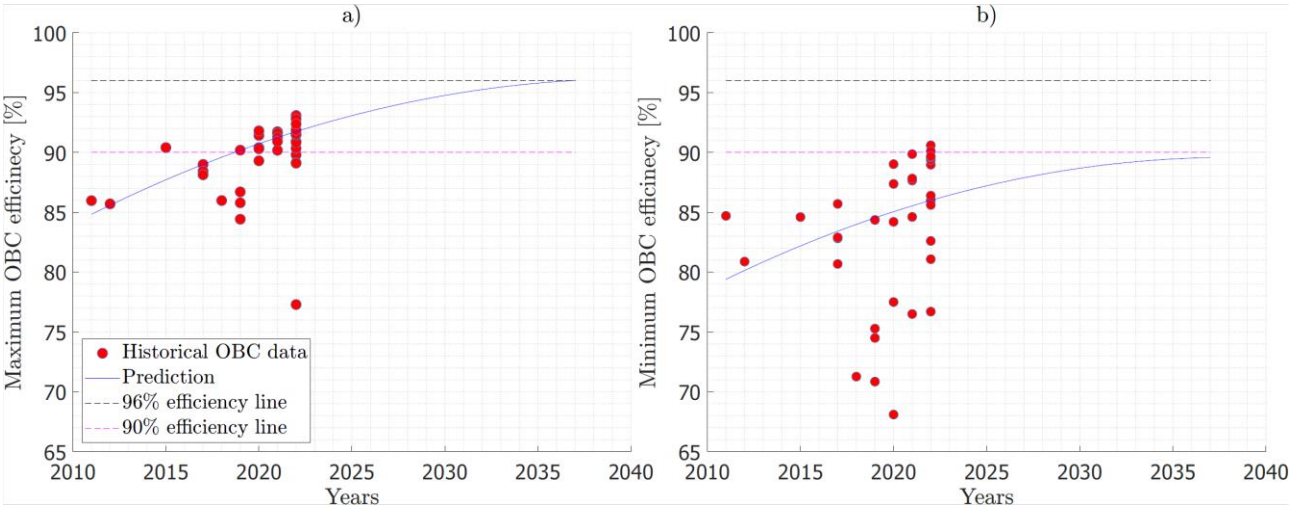


*Figure 9. Evolution of (a) maximum and (b) minimum OBC AC-to-DC conversion efficiency*

## 5.4 Development of autonomous and distributed charging technologies

In this paragraph the model and the distributed control architecture developed is described. The results of such model in two different simulated environment are illustrated.

*Figure 10* provides an overview of the control architecture. In the figure the grey shaded areas represents a number of N generic location in the distribution grid. The electricity in each area is distributed to all the connected buildings, and to the parking lots. The Cloud Aggregator (CA) performs the cloud-based global control. The Virtual Aggregator (VA), present in all the N parking lots, performs the local control architecture. The functions of the CA are the following: signal reception and processing, controllability and power set point dispatch. The CA receives signals from the grid, such as RES production from the surrounding RES power plants, and grid congestion. The CA provides controllability to different actors (Aggregator, DSOs and TSO) according to other signals (for example electricity price, or market bids). In addition, the CA provides information to parking lot users about which parking lots are available via mobile app. Users can also input through the app different requests to schedule and set their charging session priority. The users' inputs are the state of charge (SOC) at the time of plug-in, the battery capacity and the scheduled time of departure. The CA processes these inputs and dispatches to the VA both power set points and user requests.

The VA receives inputs from the CA and from the smart meter of the parking lot. On the one hand, the VA stores the user's information and schedules the charging sessions accordingly. Based on user preferences, the VA gives instructions to the chargers, such as charging priority and power scheduling based on SOC and energy charged. On the other hand, the VA of each parking lot matches the power reference given by the CA with the actual consumption recorded from the smart meter. In case there are buildings connected to the same smart meter, the VA will additionally perform power sharing between the buildings and the parking lot. For each time step, the VA broadcasts new power set points to all the chargers of its cluster.

The global control ends each iteration with a feedback loop from the smart meter to the CA. The smart meter updates the CA on the power consumed in the previous iteration. Therefore, the CA collects power consumption data from the N parking lots and redistributes the power among the parking lots according to the availability of cars and local grid conditions.

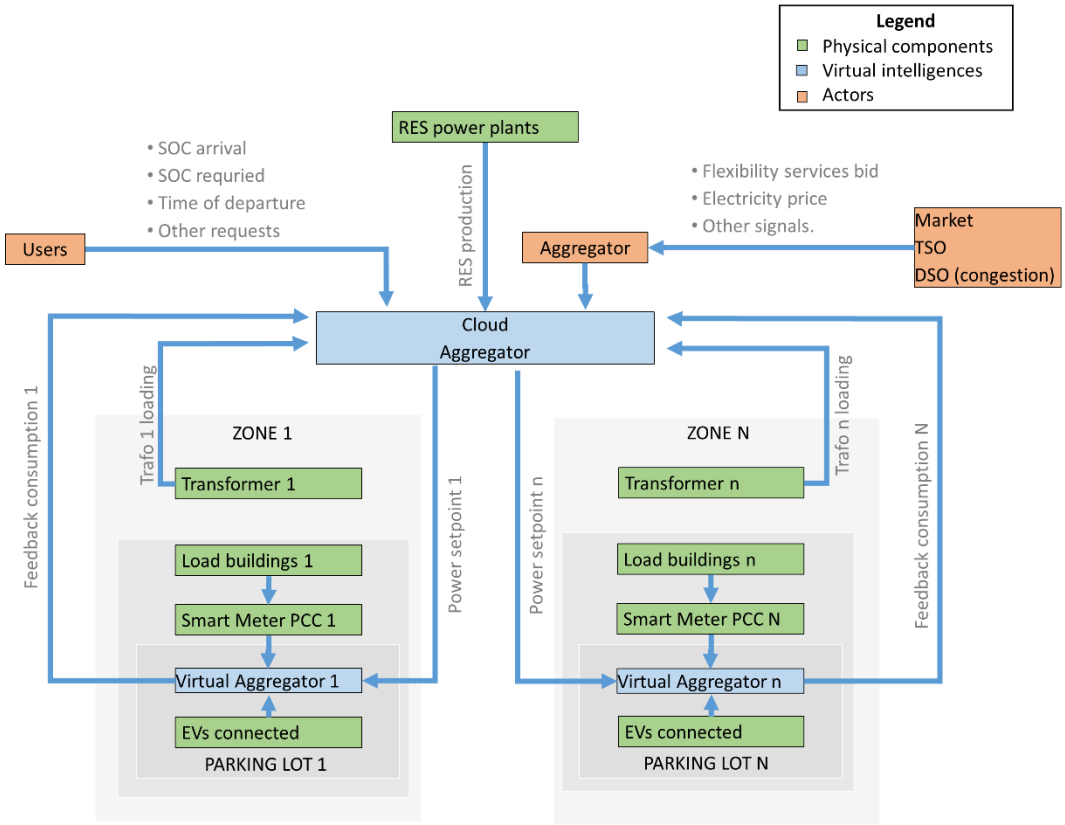


*Figure 10: Global system architecture and communication paths between different actors.*

*Figure 11*3 provides a simplified illustration of the model for a single cluster. Each charger is composed of the VA (divided into primary and secondary functions) and the charger controller. The parking lot contains N chargers. In the parking lot, there is a smart meter connected to the point of common coupling (PCC). The primary function of the VA (shortly $VA_{primary}$) is the constant power set point reception from the cloud and consequent constant adjustment of the total demand of the parking lot. $VA_{primary}$ is active only in one of the chargers, to avoid redundancy in communication. However, in case of its malfunctioning, other chargers can automatically replace it with their VA. The secondary function of the VA (shortly $VA_{secondary}$) is to schedule and share charging power among the EVs, and it is active in all the N chargers. A description of the power and information flow follows: On the left, the smart meter records the power flowing from the grid to the chargers. The smart meter sends the consumption measurements through wired communication to $VA_{primary}$, part of charger 1. $VA1_{primary}$ also receives set-points from the CA via Wi-Fi or Ethernet communication. Such set-points are the result of the CA processing data from the grid. $VA1_{primary}$ compares the difference between the set-points of the CA and the actual measurement of the smart meter and calculates an error value. $VA1_{primary}$ broadcasts the error value to all the chargers via cable (for charger 1) and via wireless communication (for chargers 2 to N).

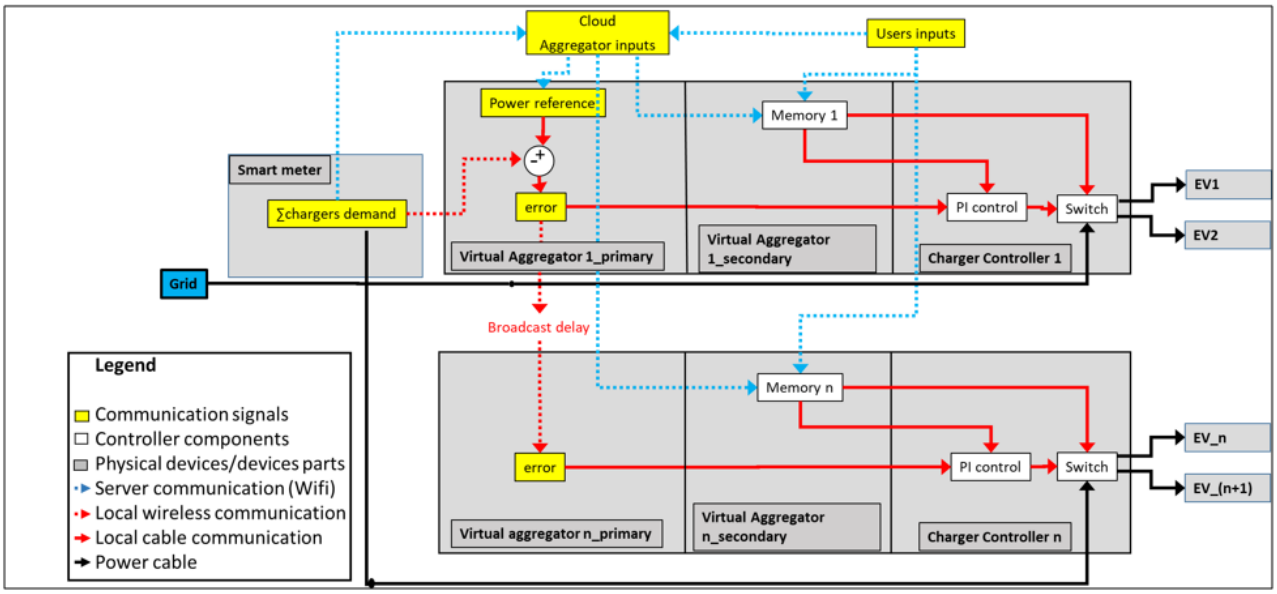


*Figure 11: Local system architectures and communication between different components of the parking lot.*

The users communicate their inputs via the mobile app to the CA. The CA sends them to the secondary function of each VA, via Wi-Fi communication. Each $VA_{secondary}$ stores the information from the charger meter and communicates with the PI control and with the switch according to the EV priorities. The power coming from the grid flows through the smart meter to the switches. The switches deliver alternately the power to one of the connected EVs based on the schedule calculated by each $VA_{secondary}$. Each $VA_{secondary}$ would automatically calculate the current SOC based on scheduled charging and user input. The total power demand is continuously recorded by the smart meter.

The model is tailored to a parking lot scenario. In details, the simulated scenario is a workplace parking lot of the Risø research campus of Technical University of Denmark. The parking lot will house 8 smart chargers with double type-2 plugs for each charger. In the model each charger can simultaneously charge only one car, even if two cars are plugged in. Each plug can support a maximum current of 16 A (11 kW charging 3 phase or 3.68 kW charging 1 phase). In the unconstrained scenario, the maximum power capacity of the parking lot is therefore 88 kW, while in the constrained charging scenario a fuse limit of 43 kW is chosen. In the latter scenario, the chargers will perform power scheduling and sharing to avoid overloading the fuse. When constructed, the parking lot will be suitable for experimental analysis to validate the results of the simulation and expand the findings to a larger scale.

### 5.4.1 One parking lot simulation

This paragraph illustrates the results of the model performance in a 1 parking lot simulation. The simulation has a total time of 24h, with a variable time-step. The inputs of the model are EV parking behavior data from a real office parking lot and are summarized in Table 2. The table shows in the same color the EVs connected to the same charger. The data are provided by a Nissan EV telematics and consist of a dataset containing arrival time, SOC at the beginning of the session, and planned departure time from 16 EV users in a time range of 24 hours with a time resolution of one second. In addition, the simulation incorporates EV models and relative battery capacity. They represent a sample of the most common EVs found in the DTU university campus. Such info is inputted in the model directly to characterize the EVs, their arrival and departure time. Based on this information the VA schedules their charging time and power.

The switch performs scheduling by prioritizing the EVs with lower SOC with schedules of 30% SOC each. The EV models contain a simplified battery model and AC-DC converter efficiency which decreases linearly from 90% at full charge (11 kW for 3 phase charging or 3.68 kW for 1 phase charging) to 80% at minimum charge (4.15 kW for 3 phase charging or 1.38 kW for 1 phase charging). At the end of each iteration, the power consumed by each charger is recorded on the smart meter. The smart meter will calculate the total power demand of the last iteration for the next iteration cycle.

Table 2. Inputs of the model for the simulation

| EV num | Model | Charging Phases | Battery_capacity [kWh] | Initial SOC [%] | Connection time [hh:mm] |
|---|---|---|---|---|---|
| EV1 | Tesla Model 3 | 3 | 75 | 25% | 08:47-18:08 |
| EV2 | Peugeot iOn | 1 | 14.5 | 17% | 09:31-12:29<br>14:41-18:00 |
| EV3 | Tesla P85D | 3 | 85 | 33% | 08:24-08:52<br>10:40-17:40 |
| EV4 | Nissan LEAF | 1 | 24 | 50% | 08:31-17:12 |
| EV5 | Nissan LEAF | 1 | 62 | 58% | 08:36-20:29 |
| EV6 | Nissan e-NV200 | 1 | 24 | 67% | 08:24-19:25 |
| EV7 | Renault Zoe | 3 | 44 | 50% | 07:47-12:15<br>12:53-16:06<br>16:24-17:18 |
| EV8 | Volkswagen E-golf | 1 | 36 | 58% | 08:15-18:10 |
| EV9 | Tesla Model 3 | 3 | 75 | 67% | 07:56-18:03 |
| EV10 | Nissan LEAF | 1 | 24 | 92% | 10:40-16:23 |
| EV11 | Nissan LEAF | 1 | 62 | 42% | 07:25-17:01 |
| EV12 | Nissan e-NV200 | 1 | 24 | 33% | 07:35-19:55 |
| EV13 | Renault Zoe | 3 | 44 | 33% | 00:21-04:00 |
| EV14 | Renault Zoe | 3 | 44 | 75% | 08:31-17:12 |
| EV15 | Tesla Model 3 | 3 | 75 | 67% | 08:55-22:16 |
| EV16 | Renault Zoe | 3 | 44 | 17% | 06:28-09:15<br>11:41-17:06 |

Figure 12 displays the connection and charging time of EVs throughout the day. The y-axis shows the EV number, while the x-axis shows the time in hours. For each EV the dotted line represents the connected time while the continuous line is the actual charging time. The lines of EVs connected to the same charger are shown in the same color. Figure 12 gives a detailed overview of the charging schedule of each EV, and the alternate switching between two EVs plugged on each charger. Further, some EVs reach their maximum SOC and stop charging before leaving. The surplus energy is used to charge the rest of EVs faster. However, the same energy surplus can be used for FTM flexibility services if the other EVs are already charging with maximum capacity.

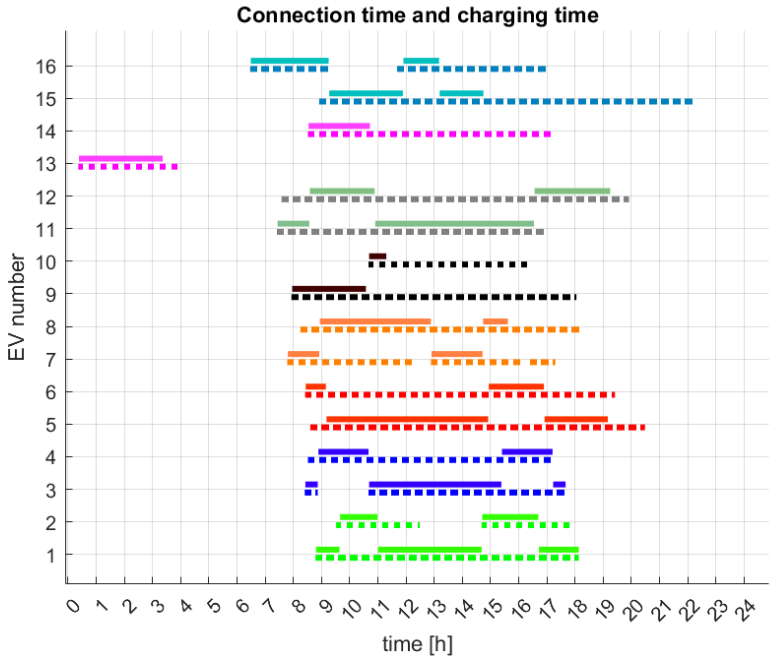


Figure 12. Connection and charging time history of the simulation

Figure 13 provides the overall results of the parking lot simulation during the 24 hours period. The top graph illustrates a time history of the charging power in the constrained charging and unconstrained charging cases for comparison. The bottom graph shows the time history of the number of EVs charging and the number of EVs connected in the constrained charging case. In the unconstrained charging case, the peak demand due to concurrent charging is 66 kW. However, the bottom graph suggests that 43 kW is an acceptable limit because most of the EVs are fully charged and stop charging long before they leave the parking lot. In fact, after 11:30 am, only 6 cars are charging at the same time.

Table 3 shows the performance of the charging sessions for the parking lot. In detail, the results are similar for both scenarios: 11 EVs are fully charged by the end of their charging session in the constrained scenario, one less than the unconstrained one. Otherwise, the results are very similar. EV11 has the lowest SOC of 78% in both scenarios. However, EV11 charges in both scenarios to its maximum power while connected, showing that constrained charging does not affect its demand fulfillment. EV11 is a single phase EV with a high battery capacity of 62 kWh and it manages to charge 25 kWh (roughly 125 km). Regarding EVs that do not reach 100% SOC: the minimum amount of energy guaranteed by the parking lot is 12.2 kWh if an EV is parked for at least 5 hours and 54 minutes. Therefore, assuming that EVs drive an average of 5 km per kWh, the parking lot is capable of guaranteeing approximately 61 km of driving autonomy during the simulated day. In addition, six of the eight chargers reach idle state for an average of 4 hours and 19 minutes per charger because their plugged EVs are fully charged. This idle time shows that, in this simulation, the fuse limit could be even lower than 43 kW without a significant effect on vehicle demand fulfillment. However, such time buffer can be used for FTM flexibility services.

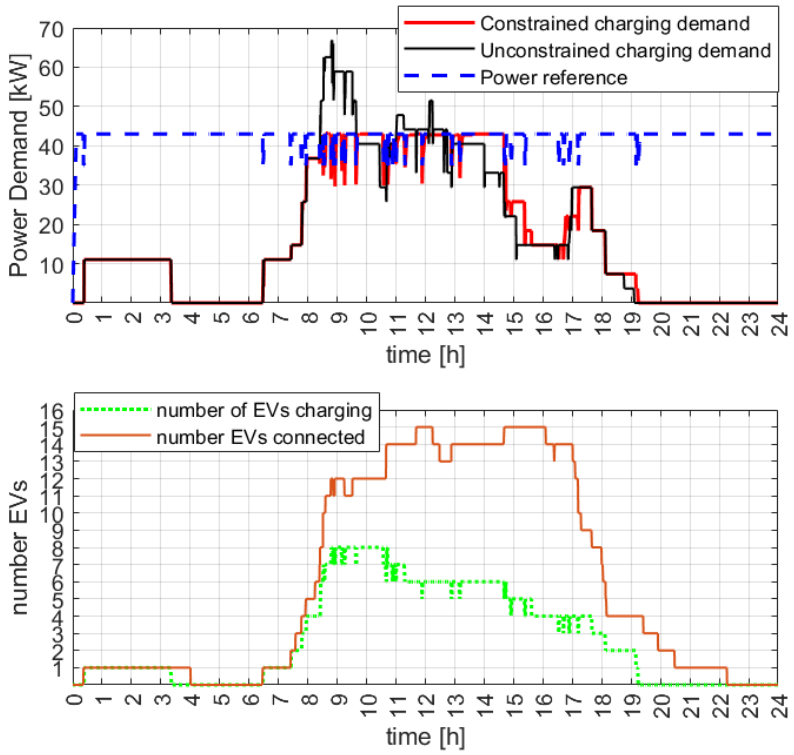


Figure 13: Overall time history of the total power demand with unconstrained and constrained charging (top). Time history of number of EVs connected and charging (bottom).

Lastly, the parking lot erogates power for 19 hours and 24 minutes over 24 hours. In such time, the total energy output in the constrained charging scenario is 414 kWh, whereas in the unconstrained charging scenario it would instead be 413 kWh. This confirms that the charging bottleneck is the power limit of each charger (11 kW, for 3 phase charging, and 3.68 kW, 1 phase charging) and not the fuse limit. The actual energy stored in the EV batteries is 368 kWh and 373 kWh in the constrained and unconstrained charging scenarios, respectively. This difference is due to the lower AC-DC conversion efficiency of the cars when modulating the charging power. These losses can be minimized by prioritizing power scheduling over power sharing. However, such losses may still be acceptable considering that the system reduces the overloading of the grid and the need to upgrade the connection capacity of the parking lot and components of the distribution grid.

Table 3: Summary of the simulation outputs

| | | Charger 1 | | Charger 2 | | Charger 3 | | Charger 4 | | Charger 5 | | Charger 6 | | Charger 7 | | Charger 8 | |
|---|---|---|---|---|---|---|---|---|---|---|---|---|---|---|---|---|---|
| Idle time constrained | [hh:mm] | 00:00 | | 00:00 | | 01:18 | | 02:32 | | 06:46 | | 00:39 | | 07:04 | | 07:30 | |
| Idle time unconstrained | [hh:mm] | 00:00 | | 00:00 | | 01:41 | | 03:28 | | 06:55 | | 00:47 | | 08:08 | | 09:30 | |
| | | EV1 | EV2 | EV3 | EV4 | EV5 | EV6 | EV7 | EV8 | EV9 | EV10 | EV11 | EV12 | EV13 | EV14 | EV15 | EV16 |
| Charging mode | # | 3 phase | 1 phase | 3 phase | 1 phase | 1 phase | 1 phase | 3 phase | 1 phase | 3 phase | 1 phase | 1 phase | 1 phase | 3 phase | 3 phase | 3 phase | 3 phase |
| Available_time | [hh:mm] | 09:18 | 05:54 | 07:24 | 08:36 | 11:48 | 00:00 | 06:42 | 09:54 | 10:06 | 05:42 | 9.6 | 12:18 | 03:36 | 08:36 | 13:18 | 08:12 |
| EV_charging_time | [hh:mm] | 05:54 | 03:18 | 05:36 | 03:36 | 08:00 | 02:42 | 02:54 | 04:48 | 02:36 | 00:36 | 6.7 | 05:00 | 03:00 | 02:12 | 04:12 | 04:00 |
| EV_tot_energy_charged_AC (constrained) | [kWh] | 59.5 | 12.2 | 58.5 | 13 | 29.2 | 8.9 | 25.6 | 17.1 | 28.1 | 2.2 | 25 | 18 | 32.4 | 13.3 | 29.4 | 41.4 |
| Final SOC unconstrained | [ %] | 99 | 98 | 97 | 100 | 100 | 100 | 100 | 100 | 100 | 100 | 78 | 100 | 100 | 100 | 100 | 100 |
| Final SOC constrained | [ %] | 96 | 92 | 94 | 99 | 100 | 100 | 100 | 100 | 100 | 100 | 78 | 100 | 100 | 100 | 100 | 100 |

### 5.4.2 VPP simulation (4 parking lots).

After the simulation on a single parking lot, the model is up-scaled to analyse the performances on large scale. For this scope in the model is integrated in the power system deployed on the island of Bornholm in Denmark. The time domain of the simulation is again 24 hours. The inputs of the simulation are SCADA secondly power production data from Kalby wind farm consisting of three wind turbines with a rated power of 2 MW. The power production is scaled by a factor of 10 before it is used as input for the simulation to match the parking lots load. The grid structure is also tailored to part of the transmission and distribution system of the island. The parking lots are connected to the 10.6 kV feeders with a rated apparent power of 500 kVA, called Kastelbakken and Rytterknægten, respectively. The model receives secondly loading data of both feeders recorded on the 20th of January 2020. Figure 146 shows the original data on wind power production and feeder loading. Notice that the feeders have two daily peaks each, during which they eventually reach values higher than 80%, which is the system's threshold for disconnecting the parking lots. This is because a safety margin of 20-30% feeders loading should always be kept in order to manage sudden spikes in demand. The EV behavior consists of pseudoreal data of 68 EVs generated from recorded data of 16 EVs by Nissan EV telematics. The dataset contains arrival time, SOC at the beginning of the session, and planned departure time from EV users. The dataset has a time range of 24 hours with a time resolution of one second. The EV models and relative battery capacity are added by the authors. They represent a sample of the most common EVs found in the DTU university campus.

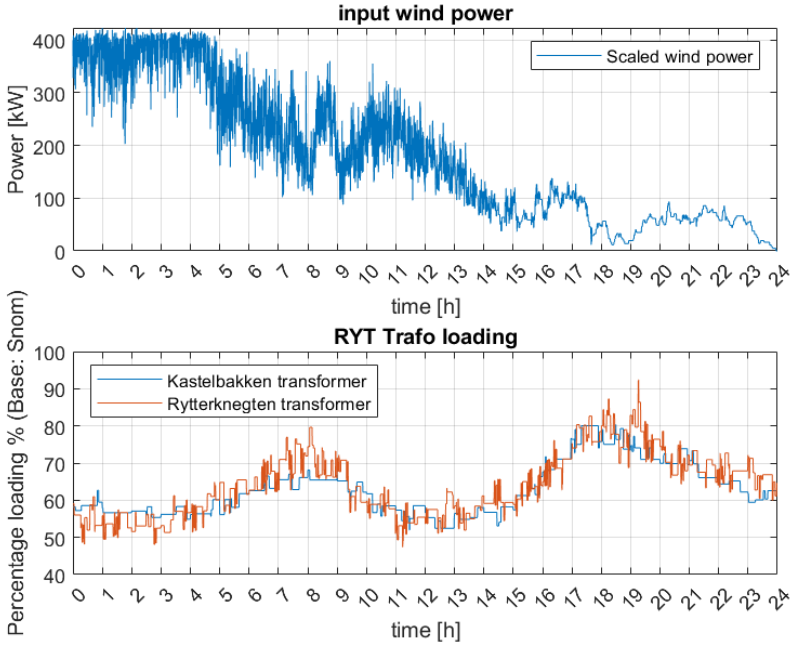


Figure 14: Top graph: Scaled wind power output of Kalby wind farm. Bottom

The model is created in Matlab/Simulink. The simulation runs with a variable time step, setting the minimum time step at 0.1 s.

Figure 14 shows the layout of the grid to which the system is applied. The system architecture controls four parking lots, two connected to Kastelbakken feeder and two connected to Rytterknægten feeder. The parking lots connected to Kastelbakken feeder house 8 and 32 EV plugs, respectively. The ones connected to the Rytterknægten feeder house 16 and 12 EV plugs, respectively.

Each of the chargers in the parking lots is equipped with type-2 plugs. Each charger has two plugs, but can simultaneously charge only one car. Each plug can support a maximum current of 16 A (11 kW charging three-

phase or 3.68 kW if charging single-phase). Each charger contains a switch, deployed to charge alternately both cars plugged according to a schedule decided automatically by the system. The schedule prioritizes EVs according to two criteria: the first is the SOC inputted by the user at the beginning of the charging session; the second is how much energy the EV charged during the current session. The priority lowers linearly as the SOC and energy charged increase. When two EVs on the same charger reach the same priority, the switch start giving power to the idle EV. One charging window lasts circa 5 kWh, but it varies marginally according to SOC and battery capacity. The VA continuously keeps track of the priority order of the cars in order to gradually disconnect the cars with the lowest priorities as the power allowance decreases. In case the feeder reaches a loading of 80% or higher all the EVs of the parking lot are disconnected. The EV models contain a simplified battery model and AC-DC converter efficiency which decreases linearly from 90% at full charge (11 kW for three-phase charging or 3.68 kW for single-phase charging) to 80% at minimum charge (4.15 kW for three-phase charging or 1.38 kW for single-phase charging).

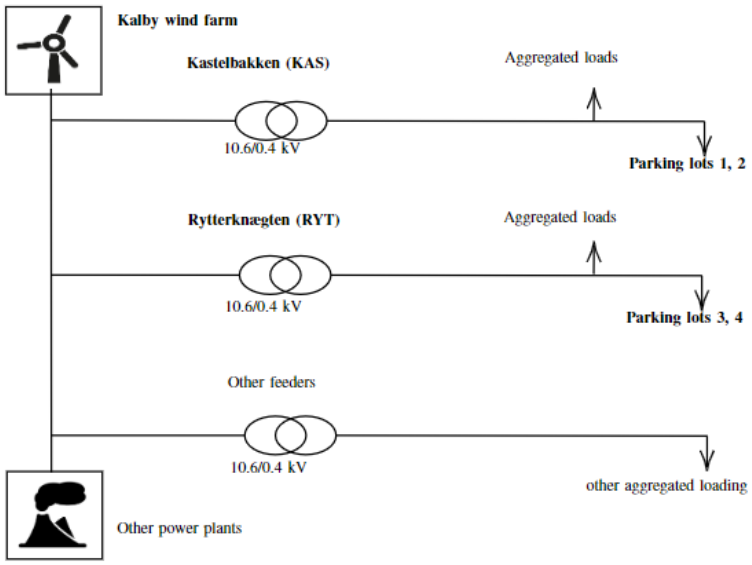


Figure 15: Simplified layout of the system

Table 4 contains the maximum power capacities for all parking lots in both constrained and unconstrained scenarios. Notice that in the unconstrained scenario, the system does not perform any power curtailment, and the maximum capacity of each parking lot is given by the power limit of the chargers, which is 11 kW. In the constrained charging scenario, the chargers adjust the power consumption to the power allowance with a PI controller. The CA instead adjusts the power set points given to all parking lots with a droop controller based on the percentage loading of the feeders.

Table 4: Maximum power for each parking lot in each scenario

| Parking lot | Unconstrained scenario | Constrained scenario |
|---|---|---|
| 1 (8 EVs) | 44 kW | 21 kW |
| 2 (32 EVs) | 176 kW | 86 kW |
| 3 (16 EVs) | 88 kW | 43 kW |
| 4 (12 EVs) | 66 kW | 32 kW |

Figure 16 provides the overall results of the simulation for parking lot 2, taken as example, during the 24 hours period. The top graph illustrates a time history of the charging power in the constrained charging and unconstrained charging cases for comparison. The graph shows in blue the dynamic power reference adjusting to the wind power and to the feeders congestion. The dynamic power reference acts as an upper boundary for the smart charging power. The power reference is controlled by the CA based on the available wind power and on transformer congestion. As expected, in both constrained and unconstrained charging scenarios, the power demand of the parking lot is lower then the power reference when there are not enough EVs available to use such power. The bottom graph shows the number of EVs connected and charging in the constrained charging scenario. When the power reference becomes too low and not all the connected EVs can charge at least with their minimum power, the EVs with the lowest priorities get gradually disconnected. From 0 to 6 am, the feeder is not loaded, therefore, the power reference equals the fuse limit. Later in the day, when the feeder becomes overloaded, the power reference is reduced, and eventually the parking lots are disconnected for safety reasons. Towards the end of the day, because of EVs leaving the parking lot, the power allowed cannot be used. As a consequence, the virtual power plant either distributes the power to other parking lots or exports it to the grid.

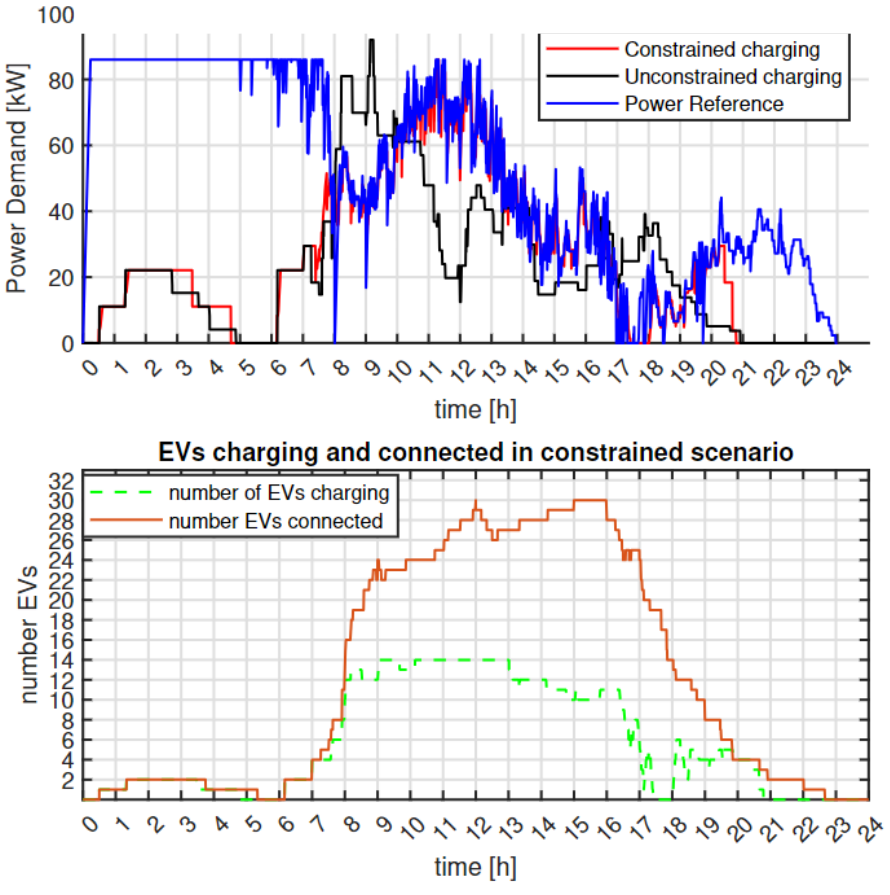


Figure 16: Parking lot 2: Power demand in constrained and unconstrained scenarios (above); Connection and charging history (below).

Figure 17 shows the distribution of energy charged for all the EVs based on their initial SOC. The graph describes that for both single-phase and three-phase EVs the system prioritizes the EVs with lower SOC and delays the charging of EVs with high initial SOC. In detail, single-phase EVs with an initial SOC lower than

60% manage to charge at least 10.7 kWh. This means that in the current conditions the 4 parking lots guarantee a driving autonomy of 53.5 km, assuming that the EVs can drive 5 km per kWh. With the current logic, the system charges three-phase EVs roughly three times more than single-phase EVs. This ratio could be decreased in order to guarantee a higher guaranteed energy charged to all EVs. However, this could potentially create discontent in three-phase EV users of the parking lot.

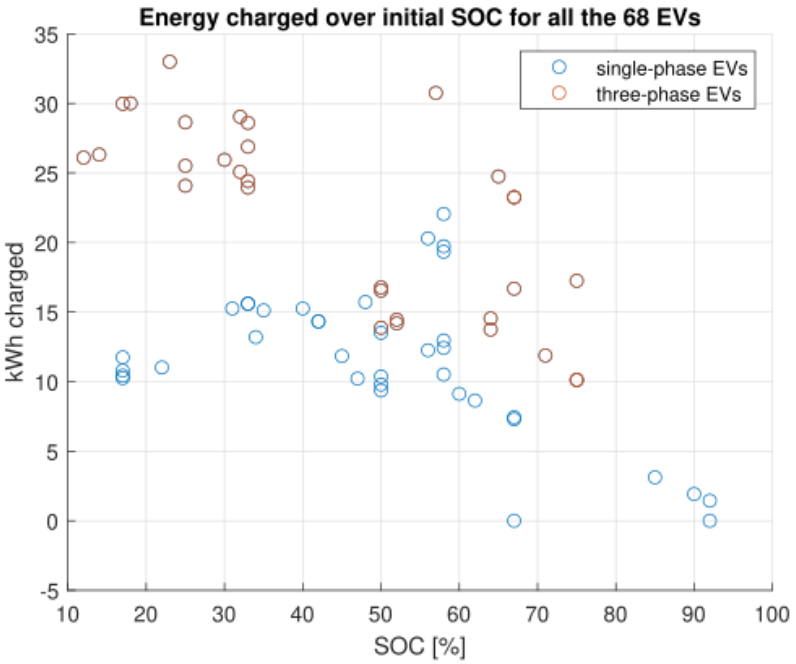


Figure 17: Distribution of energy charged over initial SOC.

Figure 18 describes the influence of parking lots on feeders and the power output of the virtual power plant during the simulated 24 hours. Both feeders (top and middle graphs) reach high-level loading (above 90%) in the unconstrained charging scenario. In the constrained charging scenario, the control architecture manages to maintain the feeder loading below the designed threshold of 80%. Notice that there are some peaks above 80%, however those peaks are present in the original data and are not due to the influence of the parking lots. The bottom graph shows the net power production of the virtual power plant, which is defined as:

$$P_{net} = P_{wind} - P_{charging}$$

Where $P_{wind}$ is the power produced by the wind farm and $P_{charging}$ is the power used by the four parking lots. The bottom graph shows also a fitting curve in order to visualize the average net power without the wind power fluctuation. In the current layout, the wind power produced is almost always higher than the power used by the parking lots. As a consequence, the virtual power plant is always exporting power to the grid.

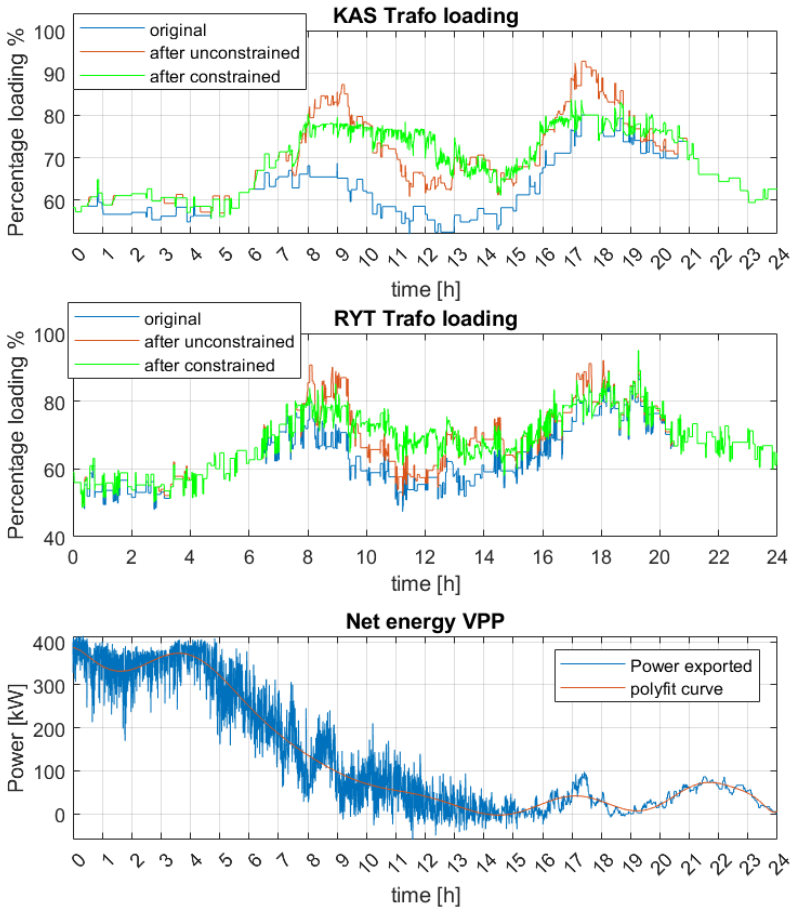


Figure 18: Overall virtual power plant graphs outputs. Top graph: Kastelbakken feeder loading. Middle graph: Rytterknægten feeder loading. Bottom graph: VPP power flow.

Table 5 presents the evaluation indices for the virtual power plant in the constrained EV charging scenario. The total energy produced during the day is 4.36 MWh of which 1.34 MWh is used to charge the EVs. The remaining 3.07 MWh is exported to the grid. A very small amount of energy (92 kWh) is imported from the grid to charge when the wind production is very low and the parking lots are full. Lastly, the average root-mean-square error provides an assessment of the wind power variability mitigation performed by the parking lots.

Table 5: Indexes of evaluation for the virtual power plant

| Index | Value |
|---|---|
| Total energy produced [MWh] | 4.36 |
| Total energy used [MWh] | 1.34 |
| Energy imported [MWh] | 0.092 |
| Energy exported [MWh] | 3.07 |

## 5.5 Architecture implementation and controller logics

According to the project objectives, the control action of the developed system is based on a distributed architecture where there is a global controller (called Cloud Aggregator) and a local controller (called Virtual Aggregator). The Cloud Aggregator (CA) is the global controller, receiving the inputs from outside the point of common coupling, performing the first layer of control, and communicating the Power set points with all the chargers. For example, it could receive inputs from RES production, Tranformer overloading, and it could also input a Power Bid in the "frequency regulation market" ($P_{bid}$). The Virtual Aggregators is the local controller, and it is assumed to reside directly inside the chargers, where each of them is controlling the power output for each plug. For the test performed by DTU however, they are located on microcontrollers outside of the chargers. The reason for this is that the microcontroller located inside of the chargers are meant to be used for the commercial application. The microcontroller used for DTU's research are shown in Figure 19.

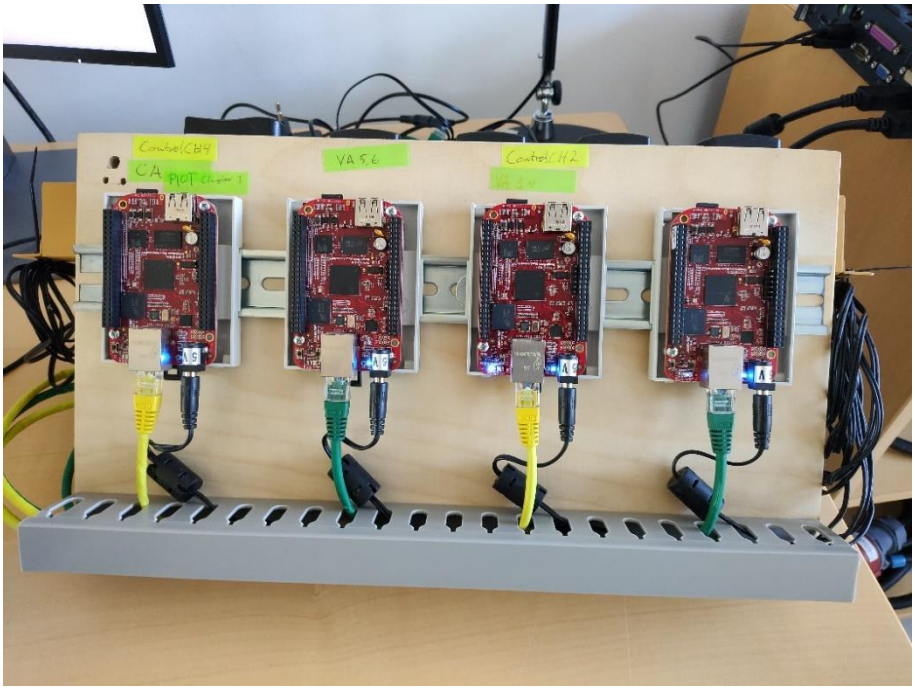


Figure 19: Microcontrollers for the CA and the VAs

The communication structure in the system is described in Figure 20:

1) The Cloud Aggregator can set the mode of communication: this could be RES following, Transformer congestion, and frequency regulation. According to the different modes, the CA will communicate continuously a power set point and the function to perform to all the VA.

2) The VAs receive the following inputs:

    a. From the CA they receive the function to perform and the power set point to follow.

    b. From the website they receive the users' inputs (time of arrival, time of departure and energy requested) to calculate the priority to give to each car.

c. They will then communicate the priority to the CA, which will share all the priorities with each chargers.

d. Lastly, all the VAs receive the Power measured at the Point of Common Coupling (PCC) from a DEIF meter.

### 5.5.1 Control in the VA

Having the above-mentioned inputs, each VA will compile the error between the Power set point given by the CA and the Power consumed by the parking lot. They will then adjust the power given to the controlled plug according to the priority given to the cars. A stronger priority results in a more aggressive VA. If a VA has a small priority, then the charging session of the corresponding user will be scheduled for later.

The two channels of communication are the whiteboard and the Amazon Web Services (AWS). These solutions are used to store and retrieve the last communication set points. The AWS is responsible for the communication between the VAs and the charger actuators, while the whiteboard is responsible for the communication between all the other components.

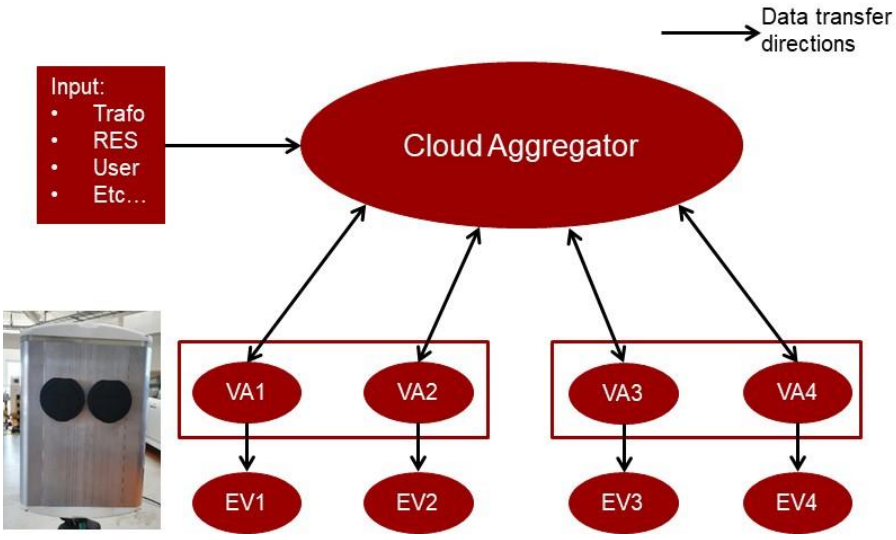


Figure 20: The system communication lines with the Control Code

## 5.6 Controllers validation in real conditions and Lab demonstration

In the following paragraphs the experimental results of the different functionalities of the system are described. Most of the results where showcased during live demonstrations organized at the PowerLab laboratory in Risø. It is important to notice that the chargers are now deployed and operated at Risø campus, at the parking lot of building 330.

### 5.6.1 Transformer Protection:

A demonstration of the capability of the architecture to adjust its charging power in order to avoid transformer overloading is presented in Figure 213.

The transformer loading limit is set to 10 kW. At 2100s RES production was shut down and thus we see no more power export (no negative values of $P_{Trafo}$) in Figure 21. The LEAF1 is connected and started to charge

at around 2200 s. At 2300 s LEAF2 is connected and since the chargers consider the EVs to charge with three phases, the first LEAF leaves space for the second diminishing the charging power. Then they both are charging at 5 kW – sharing power and without exceeding the established transformer limit.

At 2370 s an external controllable load of 40 kW is connected. The transformer has a power import spike of 50 kW. After a few seconds, the TRAFO protection mode was deployed: the EVs reacted to the transformer overloading and stopped charging to mitigate the power congestion (shown in purple circles in Figure 21. At 2410 s the external load is disconnected, thus relieving congestion of the transformer and, with an 8 s delay, the EVs started to charge again, reaching the transformer limit.

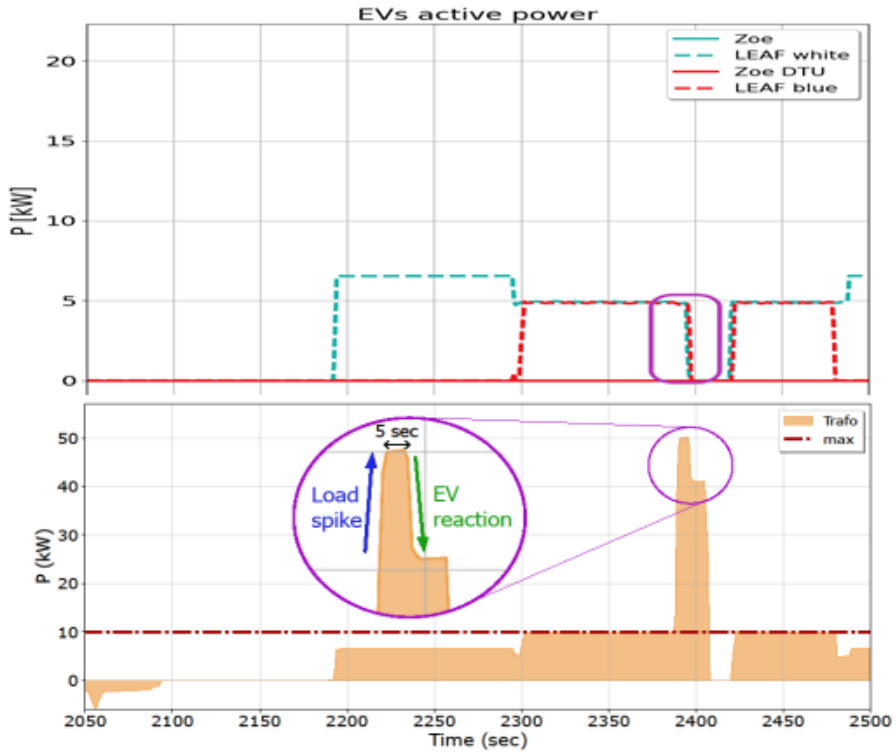


Figure 21: Active power of EVs (top plot) and at transformer (bottom plot) in the TRAFO protection test.

### 5.6.2 Power sharing mode:

The test performance can be seen from Figure 2214 with the following test description. A colour difference on the graph corresponds to different chargers (blue - C1; red - C2) and a line style - to car brand (solid - ZOE; dashed - LEAF).

The first EV – 3-phase Renault ZOE 1 - plugged to C1 at 440 s and started charging with three phases with almost maximum power of 21 kW. At 560 s a second EV – ZOE 2 - is connected to C2 and the ZOE 1 started to decrease its consumption to give space for power to the second EV to avoid overshooting the PCC limit. 10 s later (570 s) both cars were charging at the same power of 17 kW which is almost the $P_{max}$ of PCC – they are sharing the limited power between chargers.

At 690 s, a third EV – Nissan LEAF 1 capable of charging with 1-phase - is connected to C1, in response, both ZOEs decreased their consumption, and after 5 s LEAF 1 started charging 4 kW on one phase. Then, at 750 s the fourth EV – LEAF~2 connected and started to charge. We see that the cars were not charging with their maximum power. This is due to the *ghost phases* limitation. If we multiply the charging power of 1-phase cars by 3 we will see that the charging power of all EVs is actually close to the $P_{max}$ limit of PCC (36.6 kW):

$$P_{EVs} = 3\ kW * 3\ phases * 2\ EVs\ (LEAFs) + 8\ kW * 2\ EVs\ (ZOEs) = 34\ kW$$

The output power is less than the maximum due to the reactive power limitation.

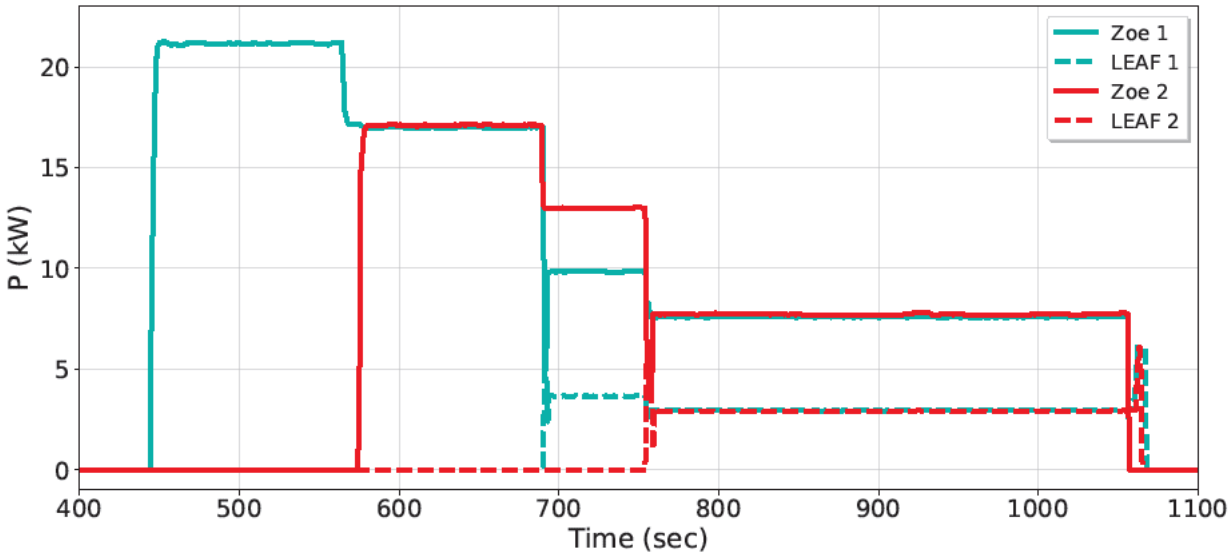


Figure 22: Power sharing test: active power of EVs

### 5.6.3 RES following mode:

A demonstration of the architecture capability to match the charging power according to RES power production is shown in Figure 2315.

The first EV – ZOE 1 is connected to C1 at 1380 s and started to charge with maximum power. The RES production is above the $P_{max}$ limit of the charger and that is why the consumption of the EV is constant. The second EV – ZOE 2 is plugged in at 1425 s and started to charge after the power sharing procedure with the first EV.

The charging power of the EVs follows the RES production with a small time delay of 5-7 s. A small discrepancy of 1.0-2.5 kW between RES production and EVs' total power consumption is again due to reactive power consumption, which increases as the power curtailment of the car increases. At 1550 s there is a steep decline in RES power production from 25 to 14 kW. The EVs reacted to that change with the above-mentioned delay within which the system was importing power from the grid to support the power balance. At 1625 s RES power again declined to 4 kW, which is now not enough to charge EVs with minimum power. So, both cars have reduced their consumption to a minimum and remained in a state of waiting for better conditions of RES production. The time sensitivity of the charger communication and control was not enough to detect and follow the RES production spike at 1675 s. At 1960 s the EVs are disconnected.

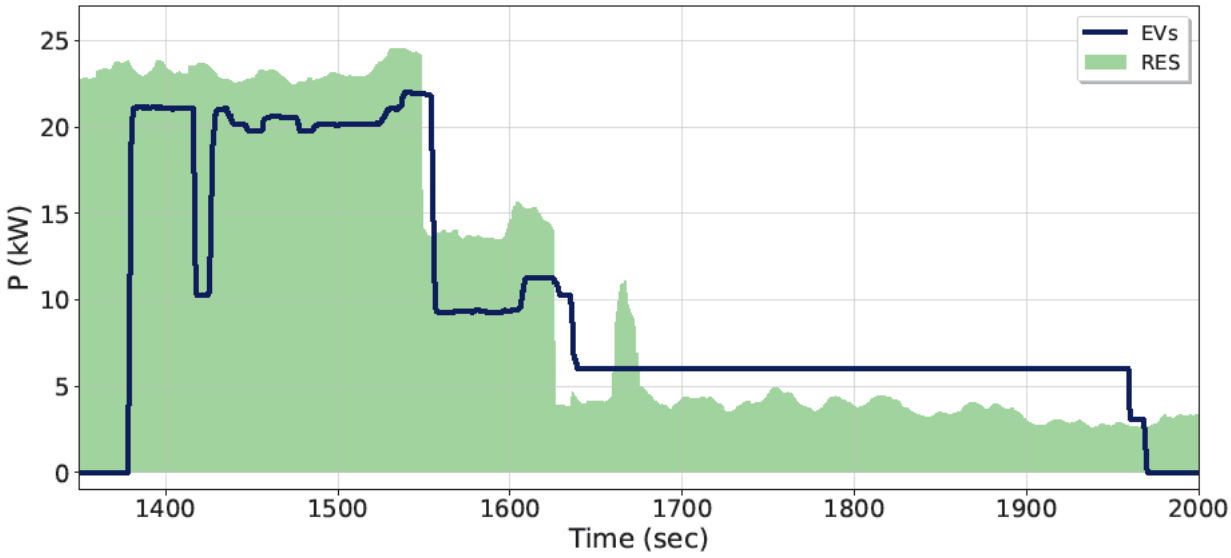


Figure 23: RES following test: total EVs active power and RES production

### 5.6.4 Frequency regulation mode:

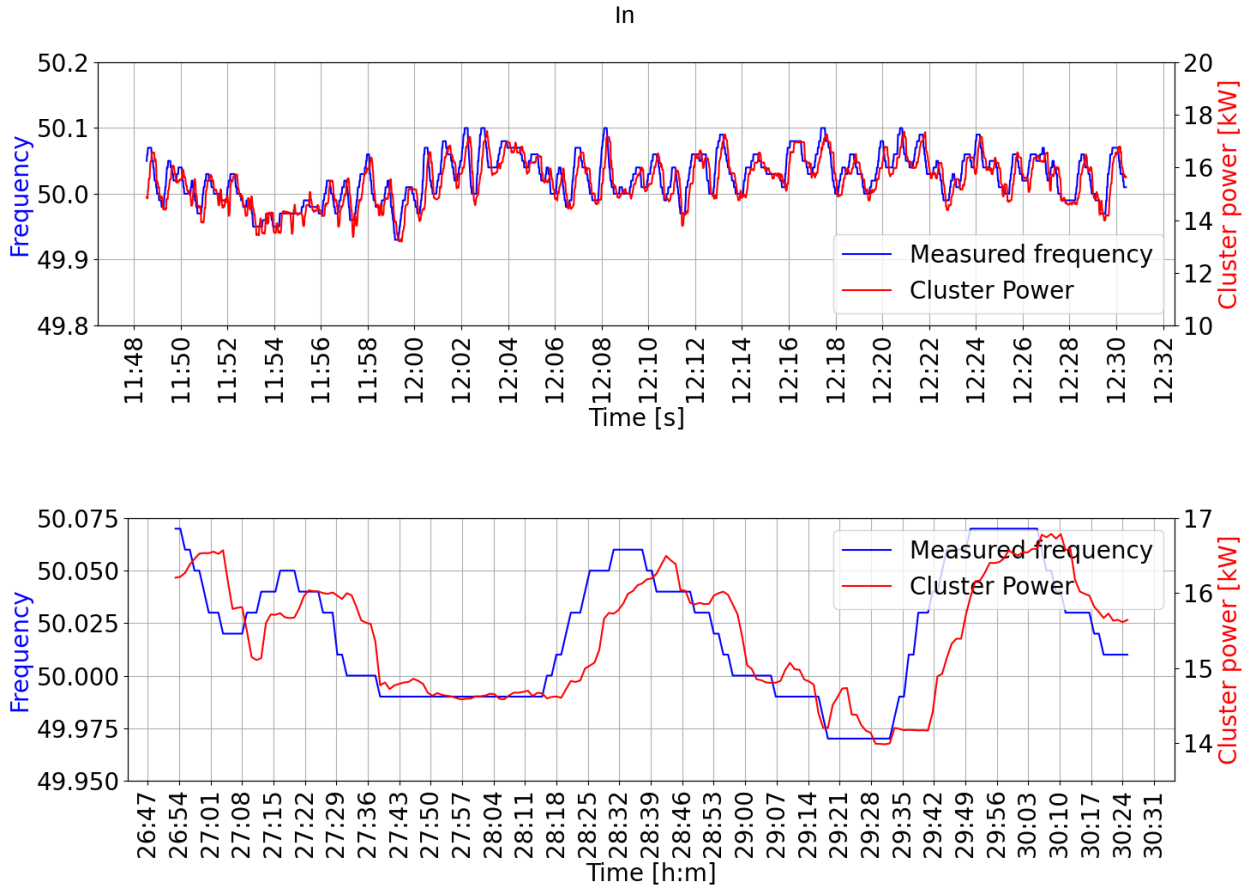


Figure 24 a time history of the frequency regulation performances is provided. The test is provided using one charger to which two Renault ZOEs are connected. In the above graph there is an overview of 1 hour ca. of frequency regulation. In both graphs the blue line represent the frequency time history, the red line represents

the power utilized by the cluster. The power adjustment is performed equally by the two EVs, as equal priority was given to them. During the test a power bid of 6 kW is provided to a hypothetical flexibility market. The droop control has a base value of 15 kW at 50 Hz frequency and offers $\pm$ 3 kW for the frequency range 50.1-49.9 Hz. The top graph shows correct and robust performances. On the other hand, the bottom graph illustrates a smaller portion of the same test, to focus on the delay of the chargers in following the frequency. The graph shows a delay ranging from 15 s to 11 s roughly. The delay depends on different factors currently under analysis: Together with the delays in communication and actuation of the control signals, an important factor is the reaction time of the cars, which is different for every brand and model.

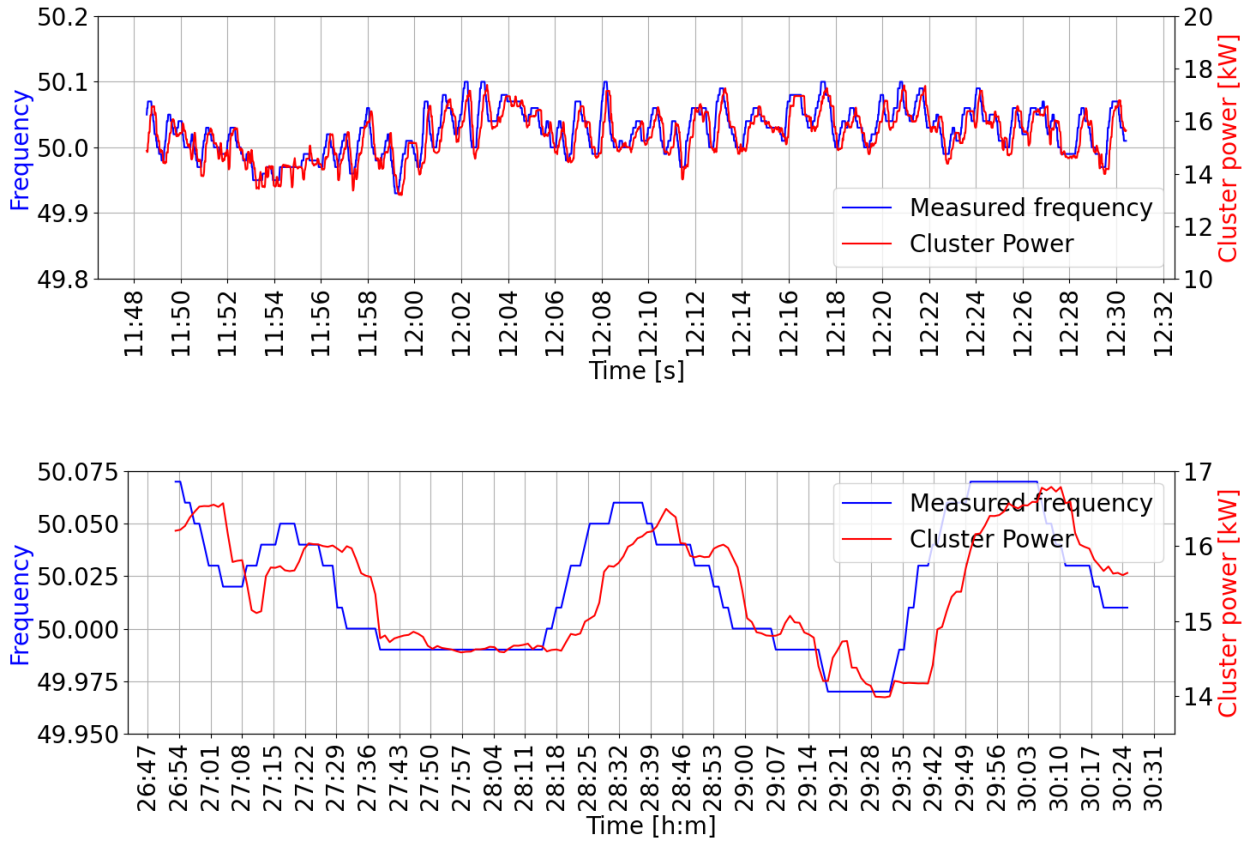


Figure 24: Frequency regulation time history. The lower plot is a zoomed instance of the above graph for better time visualization. The blue lines illustrate the frequency while the red lines illustrate the Power utilized by the cluster.

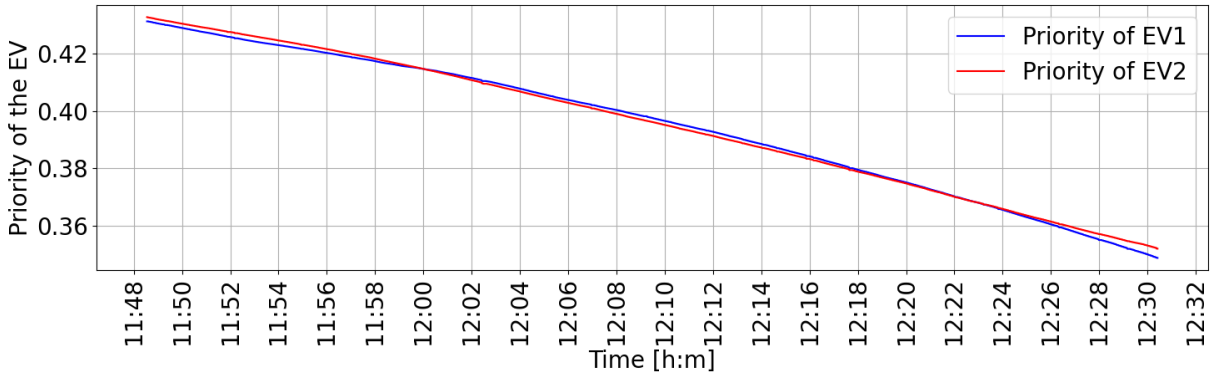

*Figure 25* and *Figure 26* show respectively development of the EVs' priority over the testing period and the power consumption of the individual EV. During the test equal priority was given to both EVs. The priority graph shows that the difference between the two cars is neglectable. However, from during the end of the test, EV2 shows a decrease in power consumption, leading to a slower decrease in priority. This behavior, although marginal, could be explained by many factors. The most reasonable hypothesis is that EV2 might be slightly undershooting the Power allowed by the chargers due to internal reason (e.g. higher SOC, different temperature etc.)

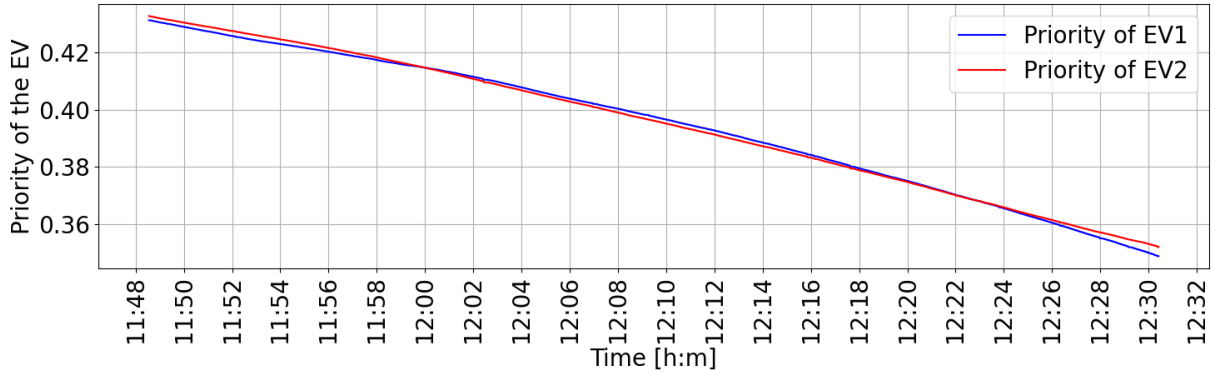


Figure 25: Time history of the priority of the two EVs during the frequency test.

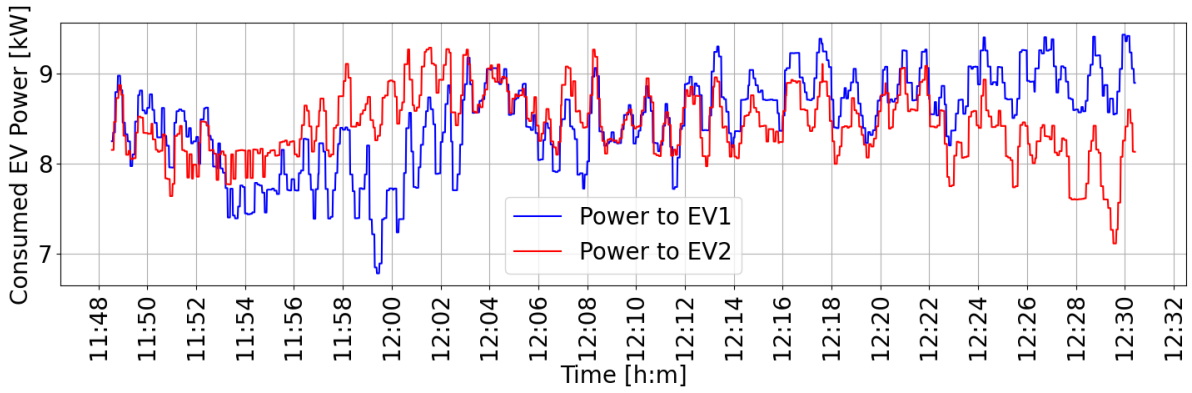


Figure 26: time history of the individual EV power consumption (bottom figure)

### 5.6.5 Scheduling and priority:

The last functionality demonstrated in the ACDC project is the capability of the developed chargers to schedule the charge between two different EVs according to the users' inputs. During the test, two cars with very similar energy request and departure time are connected to the chargers. For the scope of the demonstration the scheduling interval in the VA control is reduced to 0 s: this means that the chargers would alternate the charge to each EV as long as the priority is just marginally different. As shown in *Figure 27*, the resulting time window for each EV is therefore just a few minutes, giving the possibility to show 3 scheduling events in a small period of time. *Figure 28* illustrates the change in priority between the two EVs charging. In the graph, the first EVs starts charging: while the charging schedule is starting, the priority is 1 (the maximum priority value). When the EVs power reaches a steady state (as shown in *Figure 27*) the priority is then reduced to the priority value corresponding to the urgency of the charging session. As previously mentioned, the urgency of the charging session depends on the energy requested and by the time of departure stated by the user in our website. The visualized priority of the other EV is 0 for clarity purpose, although the real priority is memorized in the charger.

The priority of the charging EV is slowly decreasing as energy is accumulated. When the priority of the charging EV becomes lower than the priority of the other connected EV, the schedule of the second EV takes place. Therefore, the first EV stops charging, and its priority becomes 0. On the other hand, the second EV starts charging and its priority becomes 1. The cycle then continues until both charging fulfilment is reached.

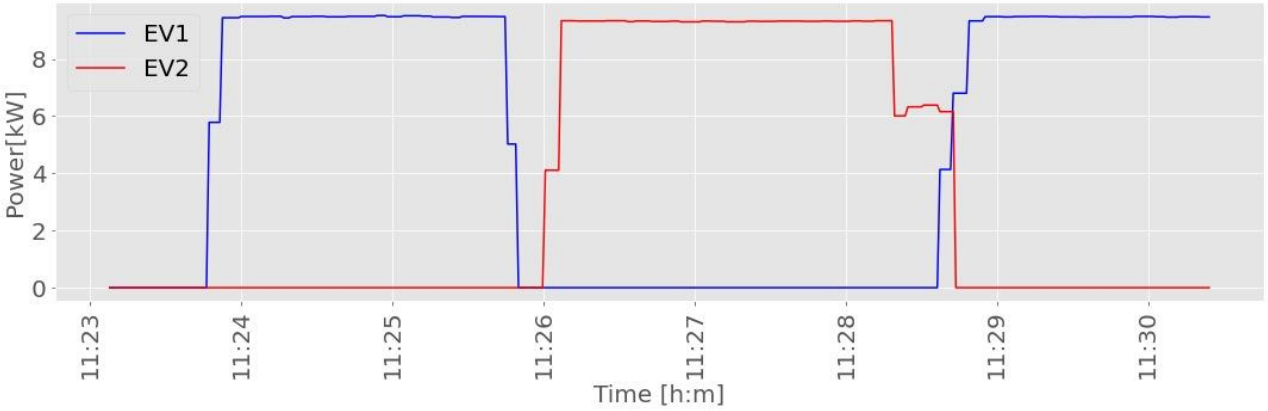


*Figure 27: Power scheduling between two EVs.*

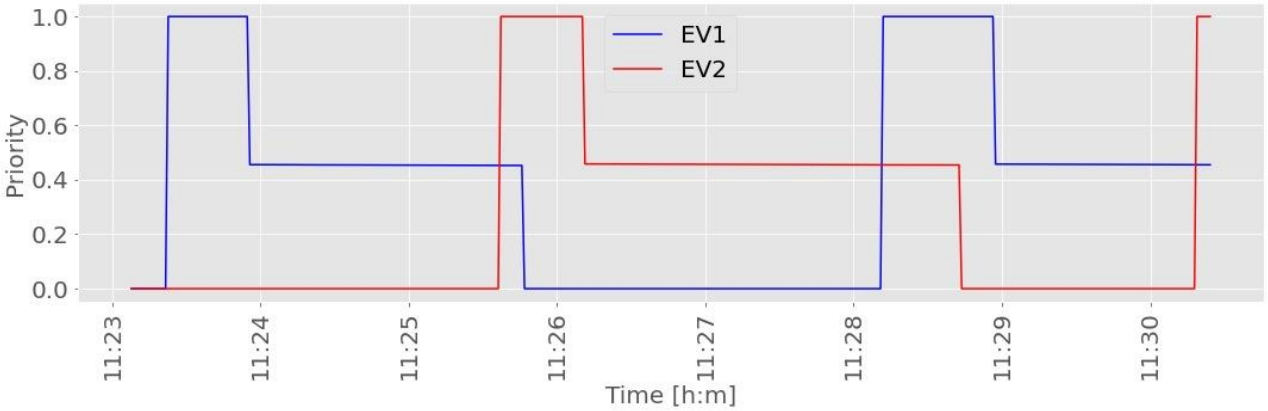


*Figure 28: Priority trend during the power scheduling test.*

# 6. Utilisation of project results

## 6.1 Overall results

During the project we successfully developed and tested an autonomous smart charging technology. It is essential to state that the test results and public demonstrations proved that the distributed control charging management system is a promising technology that enhances individual charging preferences while satisfying requirements for improving power supply safety more than a system based on centralised control.

The project efforts amounted to a total of 225 equivalent person-month (40+ people involved) over 3.5 years (April 2020 – September 2023). The overall budget was 17.7 MDKK, of which 9.0 MDKK with public support from EUDP.

Project results were collected in 29 academic peer-reviewed publications of which:

- 11 journal papers (2 currently under review),
- 12 international conference papers,
- 4 PhD theses.
- 10 master theses.

For DTU: the ACDC project supported two PhD studies (one to be completed) and reinforced the stronghold position that DTU has in the e-mobility sector both in Denmark and globally. Moreover, it allowed to gear up the activities in a new EU funded project EV4EU.

For Circle Consult: the project contributed to the development and test of a smarter, intelligent charger, potentially prepping the launch of such product in the market, creating jobs and expanding the strong point in power electronics that Denmark has.

For Nissan: The partnership with DTU and other European partners enhanced Nissan's understanding of European and Danish energy markets. Smart Charging Technologies combined with flexible energy price tariffs are not widely available in Japan. Nissan acknowledges the contribution of all the ACDC project consortium members in achieving the assumed project objectives. Despite global factors impacting the timely delivery of the project, the innovative work performed by all parties resulted in advancing the implementation of the Smart Charging Technology to the market. Finally, DTU's skills and position in the academic world are recognized by Nissan as invaluable in promoting Nissan's vision and results of past and future collaboration.

For BEOF and El-net: Several lessons were learned throughout the project. User friendliness is very important. It should be easy to see if the charger is available if the charging is in progress and when the charging session is finalized. Also, it should be visible if the charger is not charging correctly, with very few sessions not running as planned.

For Vestas: the project has contributed to successfully understanding the capability of EVs as flexible load and how to consider such capability within a hybrid power plant configuration including various generation assets.

## 6.2 Obtained technological results

The developed charging technology has been undergoing extensive lab tests since August 2022 (Figure 29) and finally demonstrated at public events in November 2022 (Figure 30) and September 2023 (Figure 31). A set of 6 chargers with 12 outlet (11 kW per outlet) has been installed at Risø facility and has became integral part of the experimental facility SYSLAB (Figure 32).


Figure 29. project partners at a project meeting demonstrating the early stage developed technology. https://www.linkedin.com/posts/mattiamarinelli_taking-smart-charging-technology-to-the-next-activity-6968863992320544769-3Y5K?utm_source=share&utm_medium=member_desktop

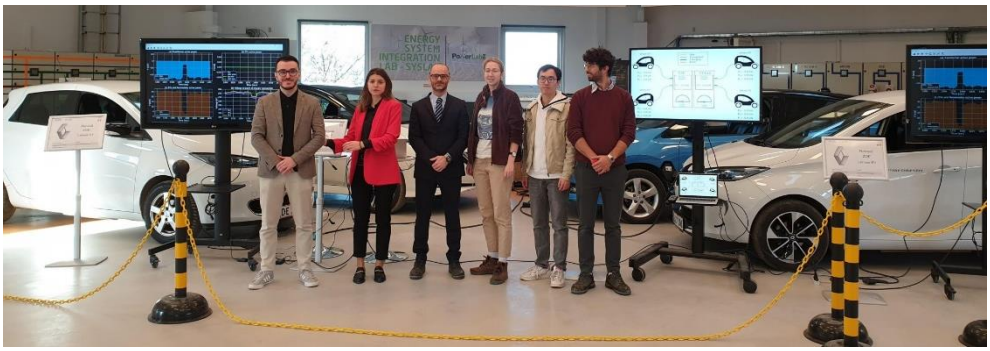

Figure 30. Public demonstration in Risø in November 2022. https://www.linkedin.com/posts/mattiamarinelli_a-superb-day-at-ris%C3%B8-with-a-smoothly-executed-activity-6996190138250723328-ExVU?utm_source=share&utm_medium=member_desktop .

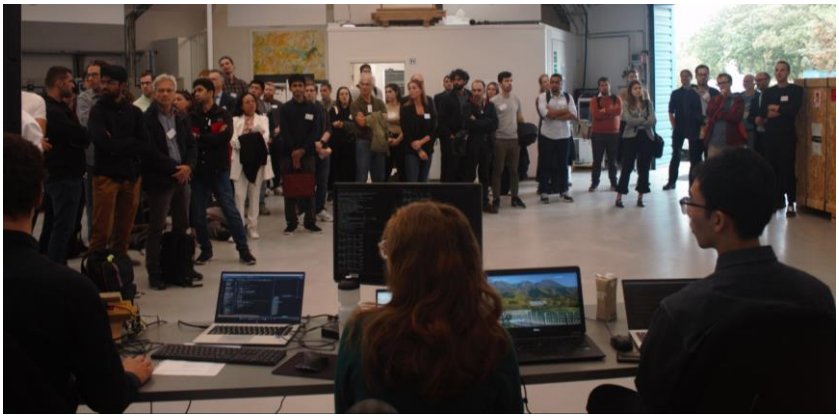

Figure 31. project partners at a project meeting demonstrating the early stage developed technology. https://www.linkedin.com/posts/mattiamarinelli_we-are-pushing-the-research-boundaries-in-activity-7111311178877816833-Jxv3?utm_source=share&utm_medium=member_desktop

Figure 32. setting of the chargers at Risø parking lot in front of Building 330.

At the demonstration site in Bornholm, one charger was installed and have been in use for a longer period of time. This charger is serving the company cars at BEOF, thus it is not available to the public Figure 33.

Figure 33. Charger installed at BEOF location.

## 6.3 Obtained commercial results

In 2022, 38% of the cars sold in Denmark was either full electric of plug in. The recent numbers for 2023 point towards 45%, full EV cars at 33%. While market demand for EV charging is clearly growing, so is supply. Several newer competitors have been found and some of these have already implemented parts of the smart charger functionality. E.g., Zaptec chargers, already in mid-2021. The number of chargers with advanced features, supporting scheduled charging and/or other “intelligent” functions, keep growing.

Additionally, the retail prices in the market are under pressure, leaving low margins, unless some central new features with significant values can be discovered and supplied. Therefore, though the current developed charger by Circle Consult, is fully functional, and feature rich, it seems unlikely that there is a clear space for this product “as-is” in the market.

The developed charger must include more functionalities to stand out and support specific niche areas of the market as a bridgehead to a larger market. Further, full cost optimization must be implemented, as the competition is leaving no room for high margins. In other words, the market seems like a red ocean, and the challenge therefore would be to find the blue spot(s) in the ocean. The work must and will continue, both in terms of market exploration and technical development, and hopefully such a spot of blue ocean will be found in the nearest future and executed comprehensively.

# 7. Project conclusion and perspective

The technological results include:

1) A 3-phase charger, behind the meter, which can be manufactured cost-effectively, thereby enabling the scaling required, to cope with the market requirements.

2) The 3-phase design provides additional instant power enabling the overhead needed for sufficiently fast charging. Thereby consuming excessive power capacity in the production.

3) The system responds to global and local requests: it therefore provides the capability to adapt to external automatic or manual data inputs (e.g. renewable production, frequency, as well as DSO and CPO and user requests).

4) The autonomous charge controller can be embedded into existing charging stations.

Fundamentally there are at least 3 elements that drive the market of State-of-the-art smart chargers:

1) Power Production fluctuation challenges – by controlling charging rate, excessive production from Solar/Wind can be prioritized (Increased charging rate) and similarly production dips can be overcome by reduced consumption (Decreased charging rate)

2) Grid overload challenges – when multiple EVs charge at same the time the current peaks on the local grid will exceed the available supply. To circumvent this will require a very costly upgrade of the local grid. Alternatively, charging must be controlled and balanced locally to match the available supply.

3) Cheaper (free) charging – while the kWh price will fluctuate the consumer will be able to charge at the time when the price is low. Or when, if charged at private premises, private production (e.g. solar panels at home) exceeds household consumption, i.e. there will be a major saving when consuming the excessive internal production for the EV charging rather than selling to the utility company.

The motivation for the deployment of a smart charger of such kind is therefore three-fold: it can be of interest to the EV producers, the grid providers as well as the EV owners.

Generally, such an autonomous charger will optimize the utilization of the invested power production capacity, thereby increasing the revenue from such investments. Furthermore, it avoids or reduces other heavy investments in infrastructure, thereby saving money. It also provides cheaper or free charging for EV owners, thereby increasing the motivation for buying EVs and helping the overall transition to electro-mobility.

As part of the Horizon Europe funded project EV4EU, the demonstration activities will continue at the parking lot located at Campus Bornholm.

# 8. References

## PhD projects connected to the project

[P1] Anna Malkova, “Electric Vehicles Powered Hybrid Power Plants,” (Alliance Ph.D. connected to ACDC and EV4EU projects), Oct. 2022 – Sep. 2025 (supervisors: M. Marinelli, J.M. Zepter, M. Korpås) https://orbit.dtu.dk/en/persons/anna-malkova

[P2] Simone Striani, “Electric vehicle clustering methods for behind the meter services”, (co-funded with FUSE), Jul 2021 – Jun 2024 (supervisors: M. Marinelli, P.B. Andersen, J. Engelhardt) https://orbit.dtu.dk/en/persons/simone-striani

[P3] Kristian Sevdari, “Control and clustering of autonomous electric vehicle chargers”, (co-funded with FUSE), Dec 2020 – Nov 2023 (supervisors: M. Marinelli, P.B. Andersen) https://orbit.dtu.dk/en/persons/kristian-sevdari

[P4] Lisa Calearo, “Grid integration of electric vehicles: battery degradation and user needs” (mainly funded by ACES/CAR/Insulae), 08/2019 – 07/2022 (supervisors: M. Marinelli, C. Ziras, R. Turri)

## Journal papers

[J1] A. Thingvad, L. Calearo, P. B. Andersen, M. Marinelli, “Empirical Capacity Measurements of Electric Vehicles Subject to Battery Degradation from V2G Service,” Vehicular Technology IEEE Transactions on, vol. 70, 2021. https://ieeexplore.ieee.org/document/9468399

[J2] A. Thingvad, P.B. Andersen, T. Unterluggauer, C. Træholt, M. Marinelli, “Electrification of Personal Vehicle Travels in Cities - Quantifying the Public Charging Demand,” e-transport, vol. 9, 2021. https://www.sciencedirect.com/science/article/pii/S2590116821000230

[J3] M. Marinelli, K. Sevdari, L. Calearo, A. Thingvad, C. Ziras, “Frequency System Stability with Converter-Connected Resources Delivering Fast Frequency Control,” Electric Power System Research. Electric Power System Research, vol. 200, 2021. https://www.sciencedirect.com/science/article/pii/S0378779621004545

[J4] C. Ziras, L. Calearo, M. Marinelli, “The Effect of Net Metering Methods on Prosumer Energy Settlements,” Sustainable Energy, Grids and Networks, vol. 27, 2021 https://www.sciencedirect.com/science/article/pii/S2352467721000904

[J5] L. Calearo, M. Marinelli, C. Ziras, “A Review of Data Sources for Electric Vehicle Integration Studies,” Renewable & Sustainable Energy Reviews, vol. 151, 2021. https://www.sciencedirect.com/science/article/pii/S1364032121007966

[J6] K. Sevdari, L. Calearo, P. B. Andersen, M. Marinelli, “Ancillary services and electric vehicles: an overview from charging clusters and chargers technology perspectives,” Renewable and Sustainable Energy Reviews, vol. 167, Oct. 2022. https://www.sciencedirect.com/science/article/pii/S1364032122005585

[J7] L. Calearo, A. Thingvad, C. Ziras, M. Marinelli, “A methodology to model and validate electro-thermal-aging dynamics of electric vehicle battery packs,” Journal of energy storage, vol. 55, Nov. 2022. https://www.sciencedirect.com/science/article/pii/S2352152X22015298

[J8] L. Calearo, C. Ziras, A. Thingvad, M. Marinelli, “Agnostic Battery Management System Capacity Estimation for Electric Vehicles,” Energies, vol. 15, 2022. https://www.mdpi.com/1996-1073/15/24/9656

[J9] K. Sevdari, L. Calearo, B. H. Bakken, P.B. Andersen, M. Marinelli, “Experimental validation of onboard electric vehicle chargers to improve the efficiency of smart charging operation,” *Sustainable Energy Technologies and Assessments*, vol. 60, 2023.

https://www.sciencedirect.com/science/article/pii/S2213138823005052

[J10] X. Cao, S. Striani, J. Engelhardt, C. Ziras, M. Marinelli, “Semi-distributed charging strategy for electric vehicle clusters,” Energy reports, 2023 https://www.sciencedirect.com/science/article/pii/S2352484723014440

[J11] S. Striani, T. Unterluggauer, P.B. Andersen, M. Marinelli, “Quantifying the impact of electric vehicle charging cluster capacity sizing on electric vehicle flexibility,” SEGAN. Under review.

[J12] K. Sevdari, P. B. Andersen, and M. Marinelli, (2023). ``Aggregation and control of electric vehicle AC charging for grid services.'' Submitted to: IEEE Transactions on Smart Grid (under review)

## Conference papers

[C1] M. Marinelli et al., "Electric Vehicles Demonstration Projects - An Overview Across Europe," 2020 55th International Universities Power Engineering Conference (UPEC), 2020. https://ieeexplore.ieee.org/abstract/document/9209862

[C2] P. Tsagkaroulis, A. Thingvad, M. Marinelli, K. Suzuki, “Optimal Scheduling of Electric Vehicles for Ancillary Service Provision with Real Driving Data,” 2021 56th International Universities Power Engineering Conference (UPEC), 2021. https://ieeexplore.ieee.org/document/9548153

[C3] S. Striani, K. Sevdari, L. Calearo, P.B. Andersen, M. Marinelli, “Barriers and Solutions for EVs Integration in the Distribution Grid,” 2021 56th International Universities Power Engineering Conference (UPEC), 2021. https://ieeexplore.ieee.org/document/9548235

[C4] L. Calearo, C. Ziras, K. Sevdari, M. Marinelli, “Comparison of Smart Charging and Battery Energy Storage System for a PV Prosumer with an EV,” ISGT Europe 2021. https://ieeexplore.ieee.org/document/9640120

[C5] K. Sevdari, L. Calearo, S. Striani, L. Rønnow, P. B. Andersen, M. Marinelli, “Autonomously Distributed Control of Electric Vehicle Charger for Grid Services,” ISGT Europe 2021. https://ieeexplore.ieee.org/document/9640132

[C6] M. Marinelli, L. Calearo, J. Engelhardt, G. Rohde, “Electrical Thermal and Degradation Measurements of the LEAF e-plus 62-KWh Battery Pack,” REST 22. https://ieeexplore.ieee.org/document/10023130

[C7] S. Striani, K. Sevdari, P.B. Andersen, M. Marinelli, Y. Kobayashi, K. Suzuki, “Autonomously distributed control of EV parking lot management for optimal grid integration,” REST 2022. https://ieeexplore.ieee.org/document/10022907

[C8] M. H. Tveit, K. Sevdari, M. Marinelli, L. Calearo, “Behind-the-meter residential electric vehicle smart charging strategies: Danish cases,” REST 2022. https://ieeexplore.ieee.org/document/10022910

[C9] K. Sevdari, S. Striani, P. B. Andersen, M. Marinelli, “Power Modulation and Phase Switching Testing of Smart Charger and Electric Vehicle Pairs,” UPEC 2022. https://ieeexplore.ieee.org/document/9917660

[C10] S. Striani, K. Sevdari, M. Marinelli, V. Lampropoulos, Y. Kobayashi, K. Suzuki, “Wind Based Charging via Autonomously Controlled EV Chargers under Grid Constraints,” UPEC 2022. https://ieeexplore.ieee.org/document/9917883

[C11] M. Marinelli, L. Calearo, J. Engelhardt, “A Simplified Electric Vehicle Battery Degradation Model Validated with the Nissan LEAF e-plus 62-kWh,” EVTEC 2023

[C12] A. Malkova, S. Striani, J. M. Zepter, M. Marinelli, L. Calearo, “Laboratory validation of electric vehicle smart charging strategies,” UPEC 2023

## Master projects

[M1] S. Bulow, T.E.H. Petersen, “A techno-economic assessment of implementing an electric vehicle and stationary storage to increase the domestic self-consumption of a prosumer with photovoltaic

installation," Bachelor thesis in general engineering, DTU, Dec 2020 (supervisors: M. Marinelli, C. Ziras, L. Calearo).

https://orbit.dtu.dk/en/activities/a-techno-economic-assessment-of-implementing-an-electric-vehicle-

[M2] I. M. Perez de Ramon, "Driving and battery degradation analysis of EVs providing frequency regulation," Master thesis in sustainable energy, DTU, Mar 2021 (supervisors: M. Marinelli, A. Thingvad, L. Calearo, H.H. Ipsen (BEOF)).
https://orbit.dtu.dk/en/activities/driving-and-battery-degradation-analysis-of-evs-providing-frequen

[M3] A. Gonzalez Delgado, "Design of electric vehicle smart charging strategies to maximize self-consumption of a hybrid power plant", Master thesis in sustainable energy, DTU, May 2021 (supervisors: M. Marinelli, J.M. Zepter, K. Sevdari, T. Gabderakhmanova, K. B. Raghuchandra (Vestas))
https://orbit.dtu.dk/en/activities/design-of-electric-vehicle-smart-charging-strategies-to-maximize-

[M4] Teis Kloster Skogland, "Charging flexibility from electric vehicles via autonomous chargers in a workplace," Master thesis Nordic5Tech, Jul 2021 (supervisors: M. Marinelli, K. Sevdari, L. Calearo, S. Striani, K. Suzuki (Nissan), V. Lakshmanan (SINTEF))
https://orbit.dtu.dk/en/activities/charging-flexibility-from-electric-vehicles-via-autonomous-charge

[M5] Elea Gwenola Marie Foulgoc, "Wind Turbine with Power Capping Capability: dynamic modelling & comparison with other power limitation methods," Master thesis in sustainable energy, DTU, Jul 2021 (supervisors: M. Marinelli, M. Ledro, J.M Zepter, K. B. Raghuchandra (Vestas))
https://orbit.dtu.dk/en/activities/wind-turbine-with-power-capping-capability-dynamic-modelling-amp-

[M6] Mari Halldis Tveit, "Electric vehicle charging flexibility for behind the meter applications," Master thesis in sustainable energy, DTU, Aug 2021 (supervisors: M. Marinelli, L. Calearo, K. Sevdari, A. Thingvad, Lauge Rønnow (Circle Consult))
https://orbit.dtu.dk/en/activities/electric-vehicle-charging-flexibility-for-behind-the-meter-applic

[M7] Vasileios Lampropoulos, "Wind farm balancing via autonomously controlled electric vehicle chargers," Master thesis in wind energy, DTU, Jan 2022 (supervisors: M. Marinelli, S. Striani, K. Sevdari, K. Suzuki (Nissan))
https://orbit.dtu.dk/en/activities/wind-farm-balancing-via-autonomously-controlled-electric-vehicle-

[M8] Bohang Shan, "Design of charging strategies with autonomous phase switching for an aggregation of EVs," Master thesis in electrical engineering, DTU, Jun 2022 (supervisors: M. Marinelli, S. Striani, K. Sevdari, K. Suzuki (Nissan).
https://orbit.dtu.dk/en/activities/design-of-charging-strategies-with-autonomous-phase-switching-for

[M9] Caroline Hørby Thellefsen and Laura Anna Lomholt, "Vehicle-to-grid services for prosumers," Bachelor thesis in Design of sustainable energy systems, DTU, Jun 2022 (supervisors: Mattia Marinelli, Jan Engelhardt).
https://orbit.dtu.dk/en/activities/vehicle-to-grid-services-for-prosumers-in-denmark

[M10] Kristoffer Laust Pedersen, "Development and testing of smart charging strategies for a workplace parking lot," Master thesis in sustainable energy, DTU, Jul 2022 (supervisors: Jan Engelhardt, Simone Striani, Xihai Cao, Mattia Marinelli)
https://orbit.dtu.dk/en/activities/development-and-testing-of-smart-charging-strategies-for-a-workpl